Universidade do Minho
Escola de Engenharia

Augusto Gonçalves Moreira

Study of design issues in a prototype lower-limb prosthesis - proof-of-concept in a 3D printed model

julho de 2021

Study of design issues in a prototype lower-limb prosthesis - proof-of-concept in a 3D printed model
Augusto Gonçalves Moreira
UMinho | 2021

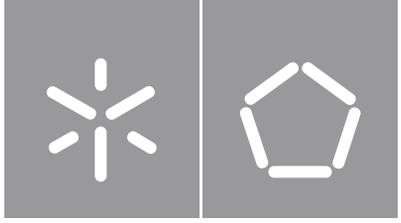

Universidade do Minho
Escola de Engenharia

Augusto Gonçalves Moreira

Study of design issues in a prototype lower-limb prosthesis - proof-of-concept in a 3D printed model

Dissertação de Mestrado
Mestrado Integrado em Engenharia Biomédica
Ramo de Biomateriais, Reabilitação e Biomecânica

Trabalho efetuado sob a orientação do(a)
Professor Doutor Eurico Augusto Rodrigues Seabra
Professora Doutora Cristina Manuela Peixoto dos Santos

julho de 2021

DIREITOS DE AUTOR E CONDIÇÕES DE UTILIZAÇÃO DO TRABALHO POR TERCEIROS

Nome: Augusto Gonçalves Moreira

Título da dissertação: Study of design issues in a prototype lower-limb prosthesis - proof-of-concept in a 3D printed model

Orientadores: Professores Eurico Augusto Rodrigues de Seabra, Cristina Manuela Peixoto dos Santos

Ano de conclusão: 2021

Curso: Mestrado Integrado em Engenharia Biomédica

Ramo de mestrado: Biomateriais, Reabilitação e Biomecânica

Acknowledgements

The present work could not have been carried out without the help and support from a great many different people.

I am thankful to my advisor, Prof. Eurico Seabra, who initially provided me with this opportunity and who helped me steer this work in a new direction once it became clear that facility and budget constraints demanded a change in course. His many friendly chats and joyful reassurances helped calm me down when panic and doubt settled in and allowed me to get back on my feet and re-focus on the work.

I must also thank my co-advisor, Prof. Cristina Santos, for lending me her seemingly inexhaustible knowledge regarding other works, projects, and opportunities that I could, and did, draw inspiration and know-how to accomplish my own goals.

I am deeply appreciative of the help provided by fellow student Joana Alves, who, despite not being obligated to do so, lent me her expertise and knowledge from having carried out the previous work on which this one builds upon. From clarifying concepts, to helping one very lost and adrift student write this very report, none of this would have been possible without her tireless help.

To the staff at Padrão Ortopédico go my sincerest thanks for meeting with me and giving me a small tour of their facilities, as well as answer my own questions regarding what patients look for in a prosthesis.

To my own family I leave a very special thanks, for all their support, help, suggestions and for believing in me, even when I didn't, and by forcing me to do so as well. They are responsible for 24 years of shaping the person I would come to be, and without them more than anyone else, I would not be who I am today.

Finally, a toast to my friends who stood by me as we faced together these last five years of university, through all the joys and hardships, and in special to Bruno, Manuel and Guillaume, the best players a tabletop game master could ask for.

Declaração de Integridade

Declaro ter atuado com integridade na elaboração do presente trabalho académico e confirmo que não recorri à prática de plágio nem a qualquer forma de utilização indevida ou falsificação de informações ou resultados em nenhuma das etapas conducente à sua elaboração. Mais declaro que conheço e que respeitei o Código de Conduta Ética da Universidade do Minho.

Abstract

The amputation of one or both lower limbs, which can be brought on by trauma, diabetes, or other vascular diseases, is an increasingly common occurrence, especially due to the increase in the number of cases of diabetes in the developed world. In Portugal alone 1300 amputations each year are attributed to diabetes. These amputations severely impact the mobility, self-esteem, and quality of life of the patients, a situation that can be alleviated via the installation of a lower-limb prosthesis. Sadly, these prostheses are not yet capable of completely emulating a sound limb in an affordable fashion.

In this dissertation, state-of-the-art research was carried out regarding the mechanics of human gait, both healthy and prosthetic. An investigation regarding the state-of-the-art research was also carried out regarding lower-limb prostheses, their evolution, mechanics, and prospects, as well as additive manufacturing techniques, and how they can be crucial to the development of affordable prostheses. Special attention was provided to the study of the leading edge of prostheses research, namely active prostheses, capable of generating and introducing energy into the human gait, rather than simply acting as passive devices.

This dissertation follows up on previous work carried out in the BioWalk Project of Universidade do Minho's BiRDLab: "Prosthetic Devices and Rehabilitation Solutions for the Lower Limbs Amputees". This work consisted of the development of an active lower-limb prosthesis prototype, with the goal of providing an affordable, but functional, prosthesis for future testing with patients. However, the resulting prototype was laden with issues, such as excessive weight and an underpowered motor. As such, this work set out to identify these issues, design, implement and test modifications to the prosthesis to produce a satisfying prototype. Given the limited resources and facilities available, it was decided to work on a smaller model prosthesis installed in a bipedal robot, the DARwIn-OP, using it as proof-of-concept for modifications to be implemented in the BiRDLab prosthesis. Modifications were successfully implemented, chiefly among them a planetary gear-based reductor and a novel attachment mechanism built using additive manufacturing techniques. It is possible to conclude that there is a great potential in the implementation of additive manufacturing techniques in the development of affordable prosthesis.

Keywords: Amputation, Gait, Prosthetic, Lower-limb active prosthesis, Additive Manufacturing

Resumo

A amputação de um ou ambos os membros inferiores, que pode ser causada por trauma, diabetes, ou outras doenças vasculares, é um evento cada vez mais frequente, especialmente devido ao aumento do número de casos de diabetes no mundo desenvolvido. Em Portugal, 1300 amputações são atribuídas aos diabetes todos os anos. Estas amputações influenciam negativamente a mobilidade, autoestima e qualidade de vida dos pacientes, mas estes efeitos podem ser minimizados através da instalação de uma prótese de membro inferior. Infelizmente, estas próteses ainda não são capazes de emular completamente um membro saudável de forma económica.

Nesta dissertação, um estado da arte do caminhar humano foi realizado, tendo em atenção o funcionamento deste, quer em sujeitos saudáveis ou amputados. Um estado da arte também foi realizado relativamente às próteses de membros inferiores, a sua evolução, funcionamento, e perspetivas futuras, e também relativamente a técnicas de fabrico aditivas e a forma como estas podem ser aplicadas em próteses acessíveis. Tomou-se atenção especial ao estudo das próteses ativas, capazes de gerar e introduzir energia no caminhar, ao invés das próteses passivas tradicionais.

Esta dissertação baseia-se em trabalho prévio ao abrigo do projeto BioWalk do laboratório BiRDLab da Universidade do Minho: "Dispositivos prostéticos e soluções de reabilitação para amputados dos membros inferiores". Este trabalho consistiu no desenvolvimento de um protótipo de prótese de membro inferior ativa, com o objetivo de criar uma prótese de baixo custo para testes em pacientes. No entanto, o protótipo produzido possuí vários problemas, tais como peso excessivo e um motor subdimensionado. Assim sendo, este trabalho propôs-se a identificar estes problemas e a desenhar, implementar, e testar modificações. Tendo em conta os limitados recursos disponíveis, decidiu-se trabalhar numa prótese modelo mais pequena, instalada num robô bipedal, o DARwIN-OP, e a usá-la para testar modificações a implementar na prótese do BiRDLab. As modificações foram implementadas com sucesso, especialmente um redutor de engrenagens planetárias e um novo método de conectar a prótese, usando técnicas de fabrico aditivas.

Palavras-Chave: Amputação, Caminhar, Prostético, Prótese Ativa de membro inferior, Fabrico Aditivo

Contents

Figure Index

Abbreviation Index

ABS - Acrylonitrile Butadiene Styrene

BiRDLab - Biomedical Robotic Devices Laboratory

BJ - Binder Jetting

CAD - Computer Aided Design

CLIP - Continuous Liquid Interface Transfer Production

DARwIn-OP - Dynamic Anthropomorphic Robot with Intelligence - Open Platform

DED - Directed Energy Deposition

DLP - Digital Light Processing

DMLS - Direct Metal Laser Sintering

DPP - Daylight Polymer Printing

EAA - Explosive Elastic Actuation

EBM - Electron Beam Melting

ESR - Energy Storing and Returning

FDM - Fused Deposition Modelling

FEA - Finite Element Analysis

FFF - Fused Filament Fabrication

FDM - Fused Deposition Modelling

LCD - Liquid Crystal Display

LOM - Laminated Object Manufacturing

ME - Material Extrusion

MJF - Multi Jet Fusion

PBF - Powder Bed Fusion

PETG - PolyEthylene Terephthalate Glycol

PKU - PeKing University

PLA - PolyLactic Acid

PPAM - Pleated Pneumatic Artificial Muscle

SEA - Series Elastic Actuator

SEAPS - Series Elastic Actuator Parallel Spring

SL - Sheet Lamination

SLA - StereoLithogrAphy

SLM - Selective Laser Melting

SLS - Selective Laser Sintering

SPARKy - SPring Ankle with Regenerative Kinetics

UM - Universidade do Minho

UV - UltraViolet

VSA - Variable Stiffness Actuation

VSO - Variable Stiffness Orthosis

VUB - Vrije Universiteit Brussel

1 Introduction

This master's thesis was developed between 2019 and 2021, in the University of Minho's Biomedical Robotic Devices Lab (BiRD Lab). This work follows a previous one, expanding upon the design and construction of a transtibial prosthesis.

Consequently, the work plan of this thesis is to continue a work integrated in the BioWalk Project of BiRDLab: "Prosthetic Devices and Rehabilitation Solutions for the Lower Limbs Amputees". This thesis addresses the development of a lower limb prosthesis, chiefly through the identification and analysis of issues and the implementation of solutions, as well as the conception and implementation of proof-of-concept ideas in a smaller prosthesis, designed to be operated by a humanoid robot, DARwIn-OP. Accordingly, this thesis represents the continuation of the work initiated by the Laboratory. In a previous master's thesis, it was conceived, designed and constructed a prototype of an active lower-limb transtibial prosthesis, with its own control mechanism [1]. This prosthesis was conceived with the following objectives and requirements in mind:

- Safety: The user must feel comfortable and confident with its motions.
- Health: Minimize the consequences of the intensive and continuous use of a prosthesis.
- Functionality: Adaptability of the human gait.
- Ergonomics: Attractive with acceptable aesthetics, adjustable to the user's anatomy while providing easy and intuitive use.
- Production: Low costs of production, ease of assembly and maintenance.

However, due to its nature as a prototype, and being the first model to be produced, this device is laden with multiple mechanical issues that render its commercialization and clinical assessment inviable. Among them we find excessive weight and an under-powered motor. Consequently, this thesis consists of the identification and analysis of these issues, and the conception of solutions. Due to the disruptions caused to normal workflow by the Covid-19 pandemic, as well as the high costs associated with prototyping and testing the components of a human-graded prosthesis, it was decided that the focus of the work should shift to the conception and implementation of proof-of-concept solutions and improvements on a smaller and lighter prosthesis, designed for use by the DARwIn-OP robot. Later, the results of this work will be valuable for the implementation of these solutions and improvements on the human prosthesis in mind.

1.1 Dissertation outline

This dissertation is organized into five chapters:

Chapter one consists of the introduction to the present work, further divided into this outline, the motivation for the realization of this work, and the goals and research questions that this work seeks to achieve and answer. Throughout this chapter, the relevant statistics are presented, as well as the causes, effects and solutions to lower-limb amputations and the issues brought by them. A brief discussion regarding the different types of prostheses and their benefits and drawbacks is also carried out.

Chapter two contains the technical review required to provide the information necessary for a better understanding of the subject matter and of the work itself. The mechanics of human gait are discussed in sub-chapter 2.1, both healthy and prosthetic, followed by a study of lower-limb prostheses, their different operating procedures, classification, and examples in sub-chapter 2.2. Sub-chapter 2.3 approaches additive manufacturing techniques, the seven different classifications that these fall under, advantages and disadvantages.

Chapter three contains the methodologies and design description, the bulk of the practical work. In their respective sub-chapters, the BiRDLab prosthesis and DARwIn-OP model prosthesis are analysed, their issues noted, and potential solutions and improvements suggested. In the case of the model prosthesis, these changes are implemented, tested, and iterated upon to arrive at the final configuration of this prosthesis.

Chapter four presents and discusses the results obtained, via the installation of the prosthesis in the DARwIn-OP robot and its operation. It is in this chapter that the answers to the research questions posed in chapter three are answered.

Chapter five concludes the dissertation, offering a short analysis of the work carried out and proposing several potential avenues for further work and research.

1.2 Motivation

The majority of lower limb amputations, around 80.9% [2], are the result of diabetes and its complications, such as infection or vascular disease with no revascularization. However, other events can also lead to an amputation, such as trauma, tumours and other vascular complications, such as acute ischemia or other acute vascular effects [2]. In Portugal alone 1300 lower limb amputations are attributed to diabetes each year. Moreover the number of new cases of diabetes has approached the 600 cases per 100 000 people mark, with elderly populations being at higher risk [3][4]. The rise in cases of diabetes may indicate an increase of lower-limb amputations, and as such, research and investment into lower-limb prostheses has also become more important. The loss of a lower limb has a massive impact on a patient's quality of life, impacting their mobility and self-esteem. Since human locomotion is a bipedal process, damage or removal of one of the lower limbs can strain movement or render it impossible, making not only activities of daily life significantly harder, but also impacting urban mobility and job opportunities. All these factors combine to potentially induce severe mental conditions, such as anxiety or depression. In fact there are studies showing that, of a sample of Portuguese amputees, 35.9% developed anxiety and 38.5% developed depression after an amputation, leading to a reduced quality of life [5].

One way to alleviate this condition is the application of a prosthesis, i.e., an artificial limb. This procedure dates back millennia, with primitive prostheses being dated as early as 300BC [6]. Like many other biomedical devices, lower-limb prostheses have been subjected to the advanced technological progress. The current leading edge is in powered prostheses, which aid in locomotion by actively mimicking the human ankle through the employment of motors that can generate work whenever necessary, rather than the traditional application of shock absorbers and springs that act as energy storing devices. These motors can mimic the power exerted by the ankle during gait, especially in the gait events where it is more needed [7]. However, these active prostheses are more expensive than passive ones, and often require the user to control them manually. Considering that many amputees are elderly, these downsides can prove to be unsurmountable, presenting a clear need, and opportunity, for a low-cost, easy to operate prosthesis. In this way, to properly contextualize the work, a state-of-the-art review will briefly cover the biomechanics of the human gait, the requirements it imposes on the project design of a potential prosthesis, the evolution through time of the different types of prostheses, their most important features and disadvantages.

1.3 Goals and Research Questions

The goals of this work can be split between the two phases of the project: the initial work being carried on the BiRDLab prosthesis, and the later work on the DARwIn-OP prosthesis.

For the initial BiRDLab prosthesis phase, the following goals were set:

- Study the development process of the BiRDLab prosthesis, its various iterations, and what issues have been previously identified, as well as noting any design flaws that may have gone un-noticed in previous work.
- Conceive potential solutions to these issues, and how viable is their implementation considering the project's budget, available facilities, and equipment.
- Implement these changes to construct a prototype of an affordable active lower-limb prosthesis that may be tested on patients for further development.

Parallel and auxiliary to the achievement of these goals, is the work on the DARwIn-OP prosthesis, which presents the following goals:

- Design, implement, and test modifications to the DARwIn-OP's prosthesis, as a proof-of-concept for further modifications to implement to the BiRDLab prosthesis.
- Prove the functionality of the prosthesis by establishing a control mechanism that will allow the DARwIn-OP to walk and balance itself.

This work seeks to, via the accomplishment of these goals, provide answers to several research questions:

- Is it possible to develop an affordable and functional active lower-limb prosthesis prototype for further testing with patients without access to expansive and expensive facilities and personnel?
- Can additive manufacturing techniques be employed to reduce the cost and time required to build and iterate prosthesis prototypes?
- Can additive manufacturing techniques produce components that have functional roles in prosthesis, or merely for aesthetic coverings and prototyping work?
- Can proof-of-concept work carried out in small bipedal robots be translated to innovations in the design and construction of prosthesis for human patients?

2 Technical Review

To properly contextualize this work, a technical review was carried out regarding the subjects of human gait, both healthy and prosthetic, prostheses, additive manufacturing, and the DARwIn-OP bipedal robot.

2.1 Human Gait

The human gait is a complex process that can be drastically altered by the presence of an injury, from a simple strain to an amputation. As such, it is important to understand the fundamental mechanics of this process, and in what ways an injury changes it.

2.1.1 Healthy Gait

The gait is a type of locomotion achieved only by the human species and through two lower limbs, thus being defined as a bipedal locomotion, i.e., biphasic forward propulsion of the centre of gravity of the human body [8]. It is a cyclic pattern, but every individual will have a slightly different gait pattern, as the specifics of one's gait vary according to various factors, such as body proportions, muscle mass, the presence of injuries, physical activity, athletic performance, and conscious efforts to alter the gait itself, among others. Over the course of a single year, the human being, in average, will take between two and five million steps. In order to maintain this level of activity, an efficient process is performed, during an healthy gait, to minimize energy requirements and reduce the chances of injury [9].

The human gait is a cyclic motion, divided into two main phases: The Stance, and the Swing. The stance phase takes up almost 2/3 of the cycle's total duration. By convention, the beginning of this cycle is defined as the moment when one of the feet contacts the ground. Then, as soon as the foot leaves the ground, i.e., is lifted, and until it impacts the ground again, it is considered the swing phase. Both phases can be further divided into sub-phases as show Figure 2.1 [10]. The stance phase can be subdivided into five events:

- **Initial contact** (i.e., heel-strike) is the moment when the heel first touches the ground and the centre of gravity of the body is at its lowest. The load begins transferring to the heel-striking foot from the opposite foot.
- **Loading response** (i.e., foot-flat) is when the plantar surface touches the ground. The load is fully transferred, and the opposite foot is lifted from the ground.
- **Midstance** occurs when the swinging foot passes the stance foot, and when the centre of gravity is at its furthest distance from the ground.
- **Terminal stance** (i.e., heel-off) happens when the heel lifts from the ground and push-off, the burst of positive power generated in the ankle joint, is initiated by the *triceps surae* muscles. The study of this phase is of special importance to this project since it is the phase where work is exerted upon the ankle to push the body forwards, thus it is the work that active prostheses seek to mimic.
- **Pre-swing** (i.e., toe-off) represents the end of the stance phase as the foot leaves the ground.

The swing phase can be divided into three subphases:

- **Initial swing** (acceleration) begins when the foot is lifted from the ground and the leg is accelerated forwards.
- **Midswing** occurs coincidentally with the opposite's foot midstance, as the swinging foot moves ahead of the stance foot.
- **Terminal swing** (deceleration) is the final phase of the swing phase, as the leg muscles slow down the leg and stabilize the foot for initial contact.

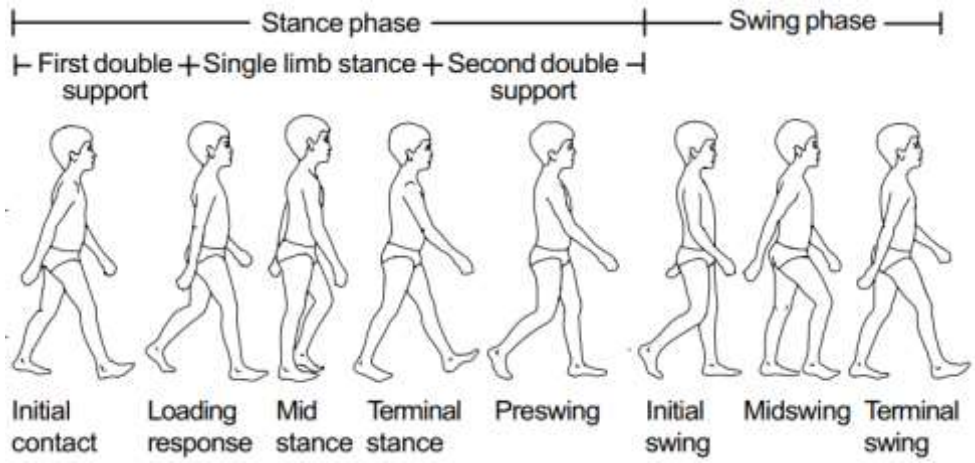

Figure 2.1 - Normal Gait Cycle [10]

Since the human moves through a bipedal locomotion, the gait involves the occurrence of two simultaneous cycles – between the left and the right lower limb, so that when one foot reaches the end of the swing phase and impacts the ground, the other one may initiate its own swing phase. In a healthy gait, these two parallel cycles will take the same time to complete, occurring with a lag of half a cycle. Gait pathologies may change this feature, as the body attempts to shorten the cycle of the injured limb as much as possible, compensating with the healthy one. This is of especial interest for this work, as the substitution of a limb with a prosthesis has a large impact on gait [10]. Figure 2.2 displays the effect that certain musculoskeletal conditions may have on the gait.

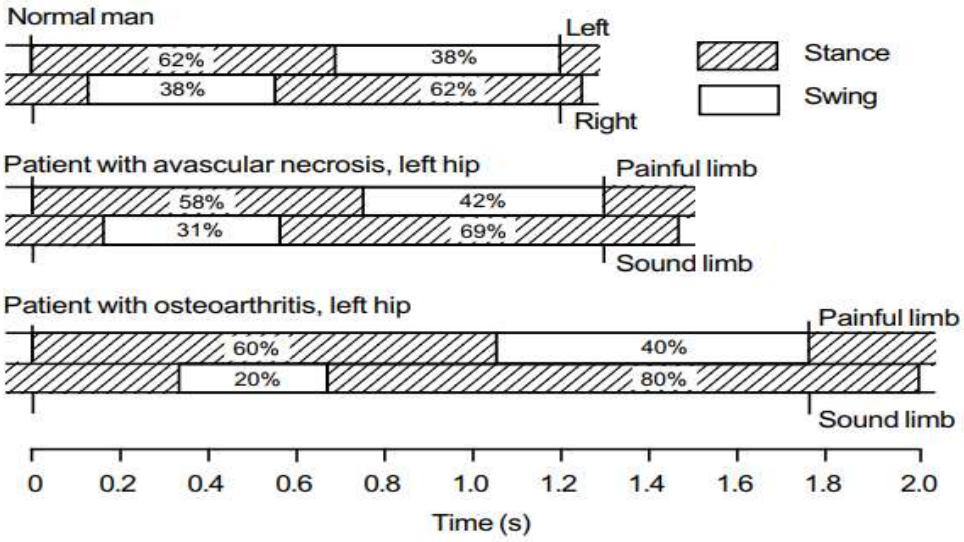

Figure 2.2 - Comparison of time spent on each limb on three different gaits [10]

Since one of the principal differences between an active and a passive prosthesis is the capability of the active prosthesis to mimic the ankle joint mechanical features, it is crucial to pay attention this joint's motion. The ankle joint is subjected to strong compressive and shear forces, while still being able to maintain a high degree of stability and being less susceptible to degenerative processes, like osteoarthritis, than other joints, such as the knee or hip. The ankle joint complex is made up of three different joints: talocalcaneal (subtalar), tibiotalar (talocrural) and transverse-tarsal (talocalcaneonavicular) [11].

These three joints combine to provide the ankle joint complex with its mobility across three planes (frontal, sagittal and transverse). On the sagittal plane, plantarflexion and dorsiflexion occur, rotating the foot up and down to provide the power for push-off. Abduction and adduction occur in

the transverse plane and inversion/eversion takes place in the frontal plane, as shown in Figure 2.3 [11]. These motions across three planes combine during gait to create pronation (movement of the foot so that the ankle leans inwards) and supination (movement of the foot so that the ankle leans outwards), which shift the weight of the body during gait, as shown in Figure 2.4 [12]. While there is a relative consensus that the majority of the work involved in dorsi and plantarflexion takes place in the tibiotalar joint, with some degrees of motion being created by the subtalar joint, no such consensus exists for the eversion/inversion movement nor for abduction and adduction, with some studies showing that both these joints cooperate to create these movements, while others show that some movements may be the exclusive purvey of a single joint [11].

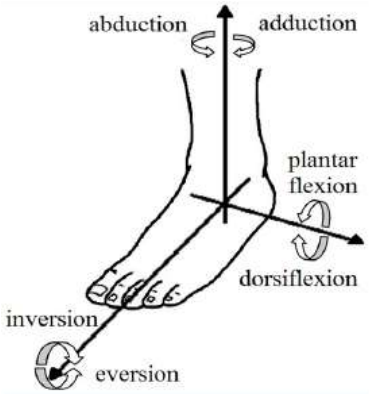

Figure 2.3 - Basic ankle movements and their axes [13]

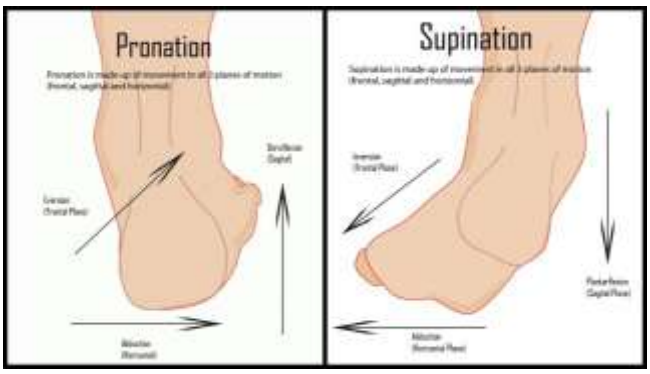

Figure 2.4 - Pronation and Supination [12]

The range of movement of the ankle varies from individual to individual, but generally it corresponds to a maximum of 20° to 30° for dorsiflexion, 40° to 50° for plantarflexion, 30° for pronation and 60° for supination, as seen in Figure 2.5.

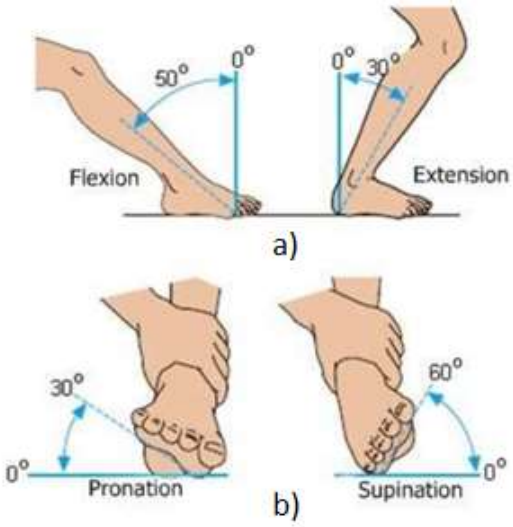

Figure 2.5 - Ranges of Motion of the ankle. a) flexion/extension, b) pronation/supination. Adapted from [13]

Different studies reach similar values regarding the maximum angles for the plantarflexion and dorsiflexion motions, regardless of whether high speed cameras or flexible sensors are used. Nonetheless, there is no consensus when attempting to measure the range of motion for inversion, eversion, abduction, and adduction, partly owed to the lack of standardization in the testing methods and definitions such as neutral positions. For example, maximum values for inversion have been measured as low as five degrees and as high as 20°, while values for eversion range from 3.6° to 14.7° [13]. Thanks to this large discrepancy in results, it is more common to study the combination of these motions and those in the sagittal plane: collectively referred to as supination and pronation. Pronation occurs during the stance phase of the gait to facilitate the absorption of impacts, provide balance and adapt to changes in ground terrain, whereas supination occurs at the end of the stance phase and sets up a rigid lever from which push-off may be initiated [14].

The rotation, position and power provided by the ankle joint complex vary during the gait cycle. Therefore, it is verifiable that in normal healthy gait the ankle does not reach the theoretical maximum range of motion, reaching only roughly 10° of dorsiflexion and 25° of plantarflexion (Figure 2.6). As expected, a spike in the power provided, of roughly 250W, is observable half-way through the cycle, corresponding to push-off, of roughly 250 W (Figure 2.7) [15].

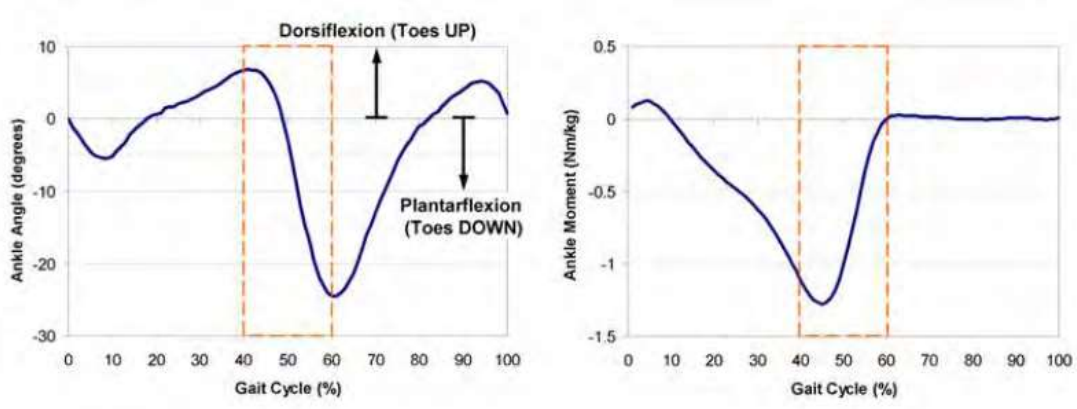

Figure 2.6 - Variation of ankle angle and ankle moment during a healthy 80kg 0.8hz human gait cycle [15]

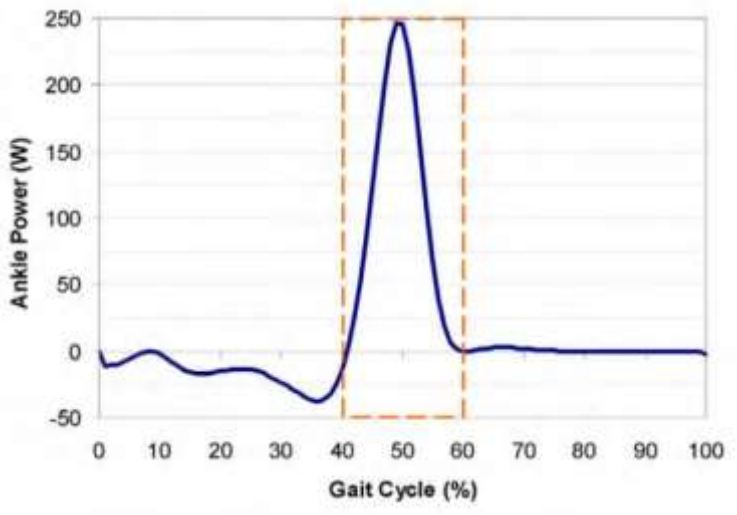

Figure 2.7 - Variation of ankle power during a healthy 80kg 0.8hz gait cycle [15]

The activity of the various muscles involved in healthy gait has also been studied extensively. For example, the *triceps surae* muscles are active during 10 to 50% of the gait cycle and provides a vital stabilizing role, whereas their antagonist, the *tibialis anterior*, is active during the swing phase and when heel-strike occurs. The *vasti* muscles are active mostly during the loading response, and the hamstring muscles, which act to decelerate the knee, reach peak activity in the latter stages of the swing phase [16][17]. The joint effort of several muscle groups and tendons is required to maintain balance and a proper gait, in a highly complex and interlocked system. To this day, the exact function and activity of several muscles are still in debate [10].

2.1.2 Prosthetic Gait

To design or improve a lower limb transtibial prosthetic device it is important to understand the unique changes in gait which these devices create upon the user, its essential use to the user's locomotion, its shortcomings, and the challenges it imposes in amputee's daily lives. The design and development process of a lower limb prosthesis is further complicated due to specific differences between the different user's physical condition and health: the stump length, the presence of muscle atrophy, and the experience and ability of the user in compensating for the differences in gait.

It is vital to consider the different types of gait movements that the patient can be expected to engage in, such as level walking, fast walking, running, ascending/descending stairs and slopes, among others. While some patients can use their regular walking prosthesis for running during short periods of time, for specialized use there are prostheses especially designed for running, mostly destined for athletes and other sports-related use [18][19]. Conventional passive prostheses struggle to provide adequate support for movement in stairs, both climbing and descending. Studies have shown that 62% of amputees with stairs in their residence can climb them independently with the aid of a handrail, while only 21% can do so without a handrail [20].

Amputees walk with 30% reduced speed and expend between 30% and 60% more energy when compared to non-amputated subjects [21]. They also experience an increased range of motion and stronger ground reaction forces on the hip joint of the sound limb, as well as increased joint moments on all joints of this limb. These factors combine to induce an asymmetric gait, which increases the risk of lower-back pain and hip osteoarthritis [22]. This asymmetry is expressed as a significant increase of the stance time of the intact limb (see Figure 2.8), as the patient is more dependent on this limb for support and propulsion. Whereas in a healthy gait the stance phase of any limb will take up roughly 60% of the total gait, in an amputee the stance phase of the healthy limb occupies 75% of the total gait, with a corresponding shortening of the swing phase of the same limb (25%) [19]. A correlation between stump length and stance phase duration has also been observed: patients with shorter stumps spend more time in stance phase and speed up the swing phase to compensate [21].

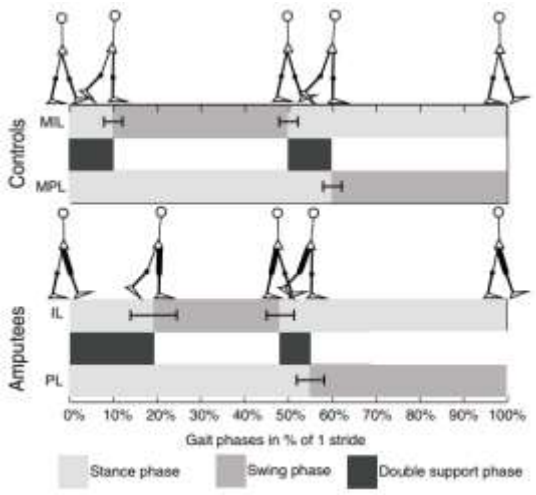

Figure 2.8 - Stride phases breakdown and comparison between a control and a unilateral amputee [25]

(MPL = mimicked prosthetic limb, MIL = mimicked intact limb, PL = Prosthetic limb, IL = Intact limb)

Amputees also tend to lean their trunk (lateral flexion) towards the amputated limb, during stance phase, more than a healthy subject (Figure 2.9). Whereas normal gait results in a symmetrical inclination of 3° to 4° towards the stance limb, the gait of amputees can display a flexion of 10° or more, as shown in Figure 2.10. A higher degree of muscle atrophy on the hip's stabilizing muscles is correlated with a higher degree of lateral flexion [21].

Figure 2.9 - Lateral flexion during amputee gait

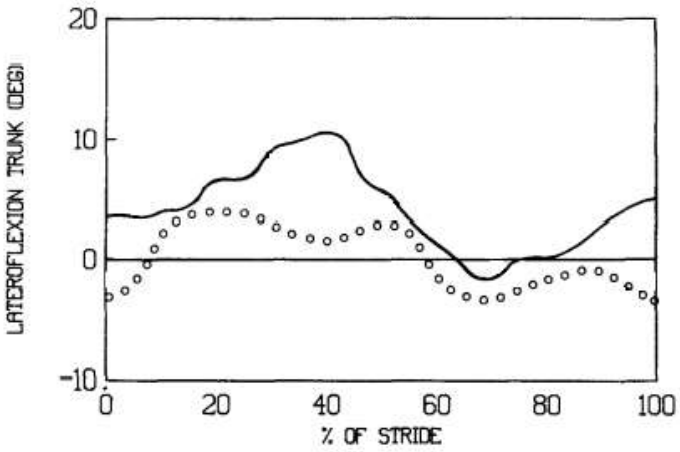

Figure 2.10 - Lateral flexion in healthy gait (dots) and in amputee gait (continuous line). Adapted from [21]

Transtibial amputees also tend to suffer from muscle atrophy, especially in the thigh muscles, which can hamper their gait. It has been found that exercises strengthening the quadriceps and hamstring results in improved gait, as these muscles act as knee stabilizers with their co-contractions. The activity of the same muscles in the intact leg is also increased, albeit not as much as those in the amputated leg, and it has been observed that the increased activity of the hamstrings results in a higher-than-normal knee flexor moment, which is countered by the co-contracting quadriceps. The proper understanding and further study of the roles of several muscles and muscle groups is vital for the development of prosthesis that are customized for the user's individual needs [17].

2.2 Prostheses

Transtibial prosthetic devices can be grouped into several categories such articulated or solid, and passive, passive with energy storing and returning capabilities or active, depending on the structure of the foot and its mechanisms, presence or absence of articulations, energy storing and energy generating mechanisms.

Passive prostheses are the oldest and simplest available, and their primary goal is to restore basic mobility. Of these prostheses, the most widespread are the Solid Ankle Cushioned Heel (SACH) feet (Figure 2.11), which are composed of a solid ankle structure, traditionally made from wood, and a cushioned heel to provide impact absorption and limited energy return. Because of their simple construction, they are cheaper and easier to maintain than other prostheses, remaining a popular option in low income countries [7]. One of their major drawbacks is the absence of an ankle joint, which leads to a poor toe-off, which in turns leads to the patient distributing more weight to the sound limb, increasing the chances of an injury [23]. To alleviate this issue, passive articulated feet are also available, the single-axis and the multi-axis foot. These prostheses possess an ankle joint which can move in the sagittal plane in the case of the single-axis foot, and in the sagittal and frontal planes in the case of the multiple-axis foot. These prostheses are more stable than conventional SACH prostheses, especially in uneven surfaces in the case of the multi-axis prosthetic. However, they are heavier and require more frequent maintenance than their SACH counterparts [24].

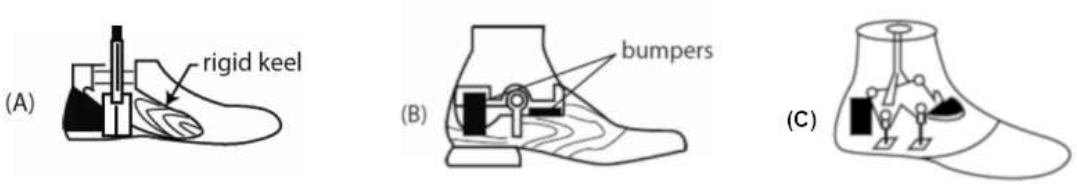

Figure 2.11 - A) SACH foot, non-articulated foot with rigid keel; B) Single-Axis foot with a sagittal joint and two flexion bumpers; C) Multi-axis foot with a sagittal and a frontal joint. Adapted from [24].

The desire of amputees to participate in sports lead to the development of the Energy Storing and Returning (ESR) prostheses (Figure 2.12, Figure 2.13), which store energy during the stance phase and return it to assist in forward propulsion in late stance. This is achieved via the incorporation of a flexible keel which compresses with the weight of the individual and decompresses later in the gait [7]. Almost 70% of patients equipped with a SACH prosthesis who transitioned to a ESR prosthesis reported improvements in gait. However, objective gait analysis revealed that the energy release occurred too late in stance, causing an alteration in the gait pattern, although the same study concluded that a propulsive force in late stance is appropriate and appreciated by the users [25]. Further studies comparing the metabolic efficiency of the SACH foot and a ESR foot concluded that at low speeds (<1.1 m/s) the differences in energy expenditure by the user were negligible. However, at higher speeds a noticeable difference in favour of the ESR foot was observed, indicating that these prostheses are more adequate for physically active patients [26], [27]. Later developments in the design of ESR prostheses sought to minimize the energy lost to friction and sound by building the shank and heel out of the same flexible material (usually carbon fibre), which allows the whole prosthesis to flex, rather than only the foot component, increasing the amount of energy stored [7].

Figure 2.12 - Össur's Variflex ESR Foot

Figure 2.13 - Össur's Cheetah Blades, ESR foot designed for running

The next step in prostheses research is the design of prostheses that can not only re-use part of the energy expended during gait, but actively generate their own power and control the release of said power so that it actively mimics the human ankle. These prostheses are known as active prostheses and represent the cutting edge of current research and development. They can be categorized based on their actuation principle as being pneumatically driven, or electrically driven [7]. Furthermore, prosthesis equipped with electronic control mechanisms that can detect human neuronal and muscular signals and use them to control the prosthesis itself are classified as bionic, and are, thanks to their advanced nature, almost universally active, rather than passive.

Pneumatic prostheses make use of pneumatic actuators to construct artificial muscles, such as the Pleated Pneumatic Artificial Muscle (PPAM), which inflate with compressed air, and allow the design of prostheses capable of producing output torques of 200 Nm, or the University of Alabama's pneumatically actuated prosthesis (Figure 2.14, Figure 2.15)[28][29]. Several devices are already commercially available that employ hydraulics to provide variable resistance in the ankle joint, such as Blatchford's Elan prosthesis (Figure 2.16). Research has also been carried out regarding the use of hydraulic actuators in an active role, and even regarding the use of rocket monopropellant to design lightweight prostheses (Figure 2.17) [30]. Despite these innovations, and their higher power/weight ratio, pneumatic actuators are less common than their electric counterparts, due to the high cost of pressurized air production and autonomy concerns [31].

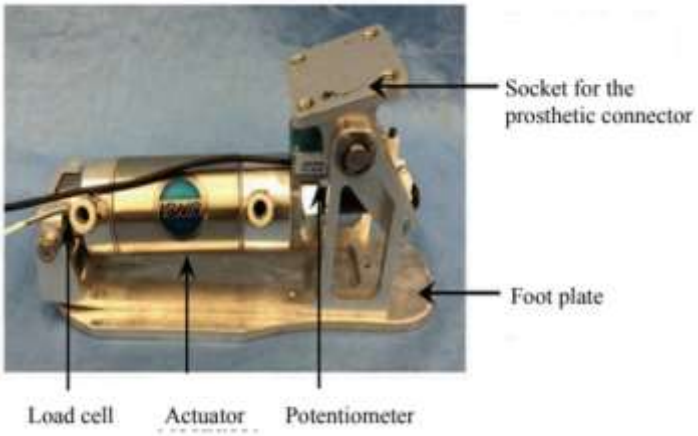

Figure 2.14 - Prototype pneumatic foot prosthesis [29]

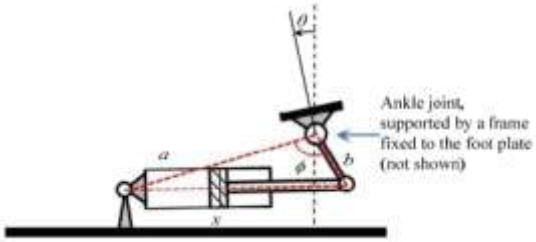

Figure 2.15 - Actuation mechanism of prototype pneumatic transtibial prosthesis [29]

Figure 2.16 - Blatchford's Elan hydraulic foot prosthesis

Figure 2.17 - Rocket Monopropellant-powered prosthesis [30]

Electrically actuated prostheses employ a DC motor to provide the power required and can be further categorized depending on the compliant actuator used, such as series elastic actuation (SEA), variable stiffness actuation (VSA), either of these actuations with a parallel spring (PS), explosive elastic actuation (EAA), among others. SEA employs a compression spring in series with the motor, requiring less power than a stiff actuator (Figure 2.18), whereas VSA employs a variable stiffness actuator, which permits the optimization of the stiffness of the joint for different walking speeds, step lengths, types of terrain, etc, at the cost of added weight and complexity. Variable stiffness actuators have been employed in both orthosis, such as University of Michigan's Variable Stiffness Orthosis (Figure 2.19), and prosthesis, such as those employed in Vrije Universiteit Brussel's Bio-inspired Biped Robot (Figure 2.20) [32][33]. The application of a parallel spring presents improvements regarding shock absorption, at the cost of energy efficiency or peak power required.

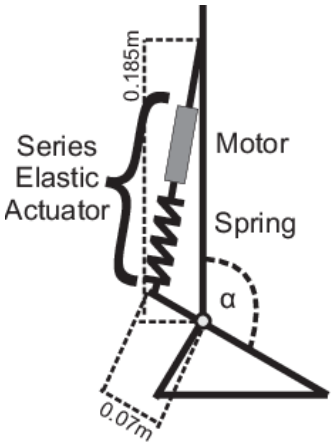

Figure 2.18 - Diagram of Series Elastic Actuator powered prosthesis [32]

Figure 2.19 - University of Michigan's VSO

Figure 2.20 - VUB's VSA [33]

EAA is a novel type of actuation which makes use of a loaded spring behind a locking mechanism in series with a SEA, delivering an explosive burst of power at the required instant, which is especially useful in activities such as jumping, kicking, throwing, etc. One device that makes use of such technology is the AMP-Foot 3, as seen in Figure 2.21 [34].

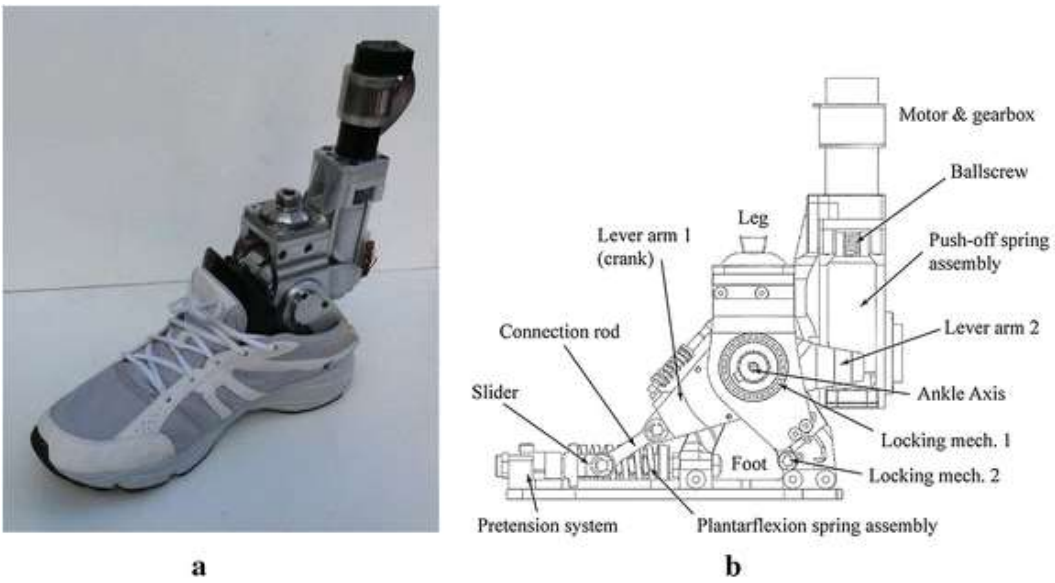

Figure 2.21 - a) AMP-Foot 3; b)AMP-Foot 3's components [34]

SEA and SEAPS are the most used mechanisms, since they lower the required peak power without wildly increasing complexity [31]

Some other examples of prosthesis that are in active research or already commercially available include the PKU-RoboTPro (Figure 2.22) and the SPARKy prosthesis (Figure 2.23) [35][36]. To date, there are very few bionic prostheses available for commercialization due to many issues such as cost, autonomy, weight, and maintenance requirements. Examples of such prosthesis include BionX's EmPOWER ankle (Figure 2.24) and the iWalk BiOM [37].

Figure 2.22 - PKU-RoboTPro prototype, adapted from [35]

Figure 2.23 - SPARKy 3 prothesis fitted to a patient [36]

Figure 2.24 - BionX's EmPOWER ankle [37]

2.3 3D printing/Additive Manufacturing

3D Printing, also known as Additive Manufacturing, is the construction of a three-dimensional object, in a layer-by-layer fashion, from a CAD model or a digital 3D model. In the 1980's, this technology was considered only adequate to produce functional or aesthetic prototypes, and was more commonly known as Rapid Prototyping, but more recent, rapid improvements in precision, repeatability, and range of available materials have rendered it a viable as an industrial-production technology [38].

Additive Manufacturing presents several advantages over traditional manufacturing techniques, chiefly among them: the ability to produce simple components as well as complex ones, not requiring large and complex production facilities, not requiring in-depth knowledge to

operate, shorter product development cycles, reduced manufacturing costs, the ability to directly print complex structures that would otherwise require assembly, less constraints imposed on the design by the manufacturing process than traditional manufacturing processes, among others [38][39]. It does possess some disadvantages when compared to traditional manufacturing techniques, such as printed pieces not achieving the same standards of performance, low precision, limitations in surface finish, the need to print support material in certain conditions, and large variations in the properties of printed components [39].

Additive manufacturing processes can be divided into seven categories, depending on the specific technology and methodology that they make use of. These categories are binder jetting, material extrusion, directed energy deposition, material jetting, powder bed fusion, sheet lamination and vat photo-polymerisation [40].

2.3.1 Binder Jetting

Binder jetting consists of applying a layer of binding solution on a powdered material with a jet. Multiple layers of powder and binding solution are applied to get the desired product. This technique can be used with a variety of raw materials, such as ceramics, composites, metals, and polymers. It is a relatively inexpensive and fast technique but produces poor surface finishes and fragile parts when compared with other methods, such as directed energy deposition (Figure 2.25) [41].

Figure 2.25 - 6 Stages of Binder Jet 3D printing [42]

2.3.2 Material Extrusion

Material extrusion consists of heating the material into a semi-solid state, and extruding it onto a defined path, building the object layer-by-layer. A filler material may be used to support the parts as they print and can be easily removed afterwards (Figure 2.26). This technique is inexpensive, but can only operate with ceramics and polymers, and the parts suffer from a "staircase" effect, anisotropy, between layers. Some of the most used polymers include PLA (Polylactic Acid), ABS (Acrylonitrile Butadiene Styrene) and PETG (Polyethylene terephthalate glycol), each with their own properties that render them more adequate to specific functions. One of the most popular 3D printing methods is a material extrusion technique trademarked by Stratasys, under the name of FDM (Fused Deposition Modelling), but there are others, such as FFF (Fused Filament Fabrication). These techniques vary only in name, as FDM is a trademarked term, whereas FFF is not, but they are functionally identical [43].

Material extrusion is of particular interest, as it was used extensively throughout this work. This technique has become much more accessible to the public, with (relatively) low costs for printers and materials, ease of use, and large availability of tutorials, models, and other resources for public consumption.

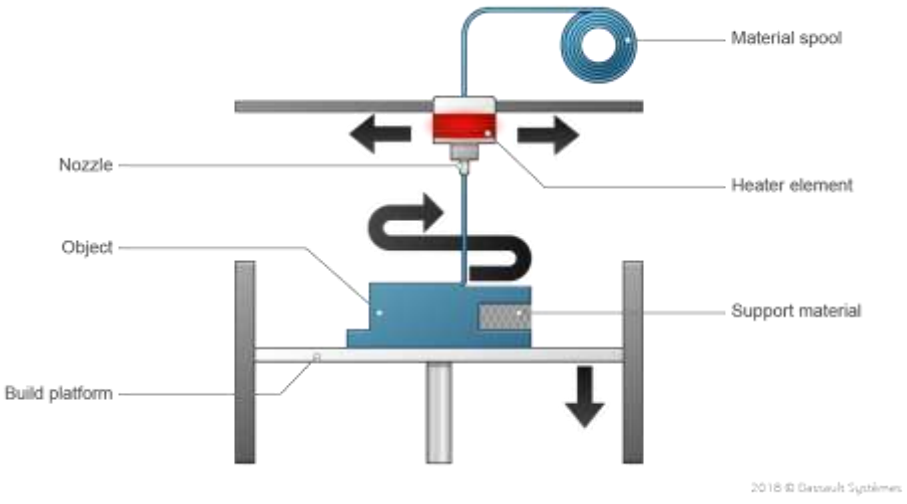

Figure 2.26 - Diagram of Material Extrusion [44]

2.3.3 Directed Energy Deposition

DED makes use of the same principles as material deposition, but the nozzle has multiple degrees of freedom, which allows for a higher-quality surface finish, at the cost of speed. It can employ metals and hybrids as raw materials (Figure 2.27) [40].

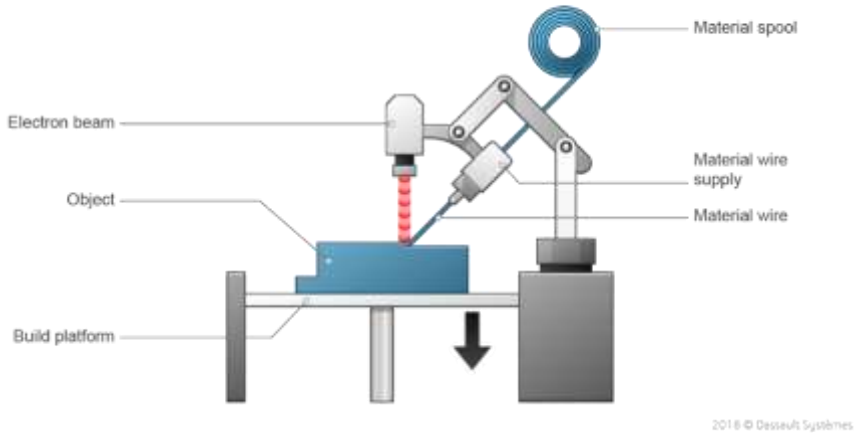

Figure 2.27 - Diagram of Directed Energy Deposition [44]

2.3.4 Material Jetting

In Material Jetting, a dispenser drops small droplets of the material, or jets it, onto the build the surface, which solidifies under UV light. However, only a few materials can be manipulated in this way, which translates into a limited selection range. The final product is of high quality and has a good surface finish (Figure 2.28) [45].

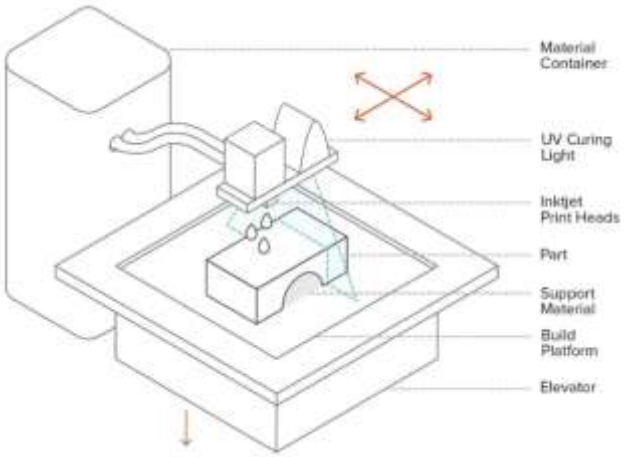

Figure 2.28 - Diagram of Material Jetting [45]

2.3.5 Powder Bed Fusion

In Powder Bed Fusion, an electron beam or laser melts the powdered raw material together, forming structures quickly and accurately, and without the need for support material. Furthermore, leftover powder from a print may be re-used, reducing costs. Multiple methods of Powder Bed Fusion are available, such as Selective Laser Sintering (SLS), Selective Laser Melting/Direct Metal Laser Sintering (SLM/DMLS), Electron Beam Melting (EBM), and Multi Jet Fusion (MJF), among others. These methods differ in copyright, specific operations, and materials, with SLS using primarily polyamide and alumide as raw materials, whereas DMLS uses powdered metal. Meanwhile EBM fuses the powder with an electron beam rather than a laser, and MJF uses an inkjet array to apply fusing agents that are heat fused into a solid layer (Figure 2.29). The largest downside of Powder Bed Fusion methods is a higher energy consumption and a low quality surface finish, as well as the need for post-processing via an airbrush, to remove leftover powder and other binding agents [46].

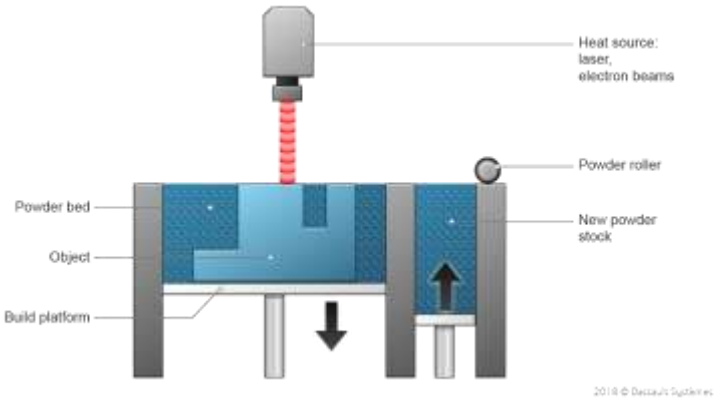

Figure 2.29 - Diagram of Powder Bed Fusion [44]

2.3.6 Sheet Lamination

Sheet lamination, also known as Laminated Object Manufacturing, forms structures by stacking layers of foil material, cutting them to shape with a laser or blade, to fit the object's cross-section, and sticking them together with an adhesive. Initially this method operated exclusively with paper as a material, but new materials are now available, such as fibre-reinforced composites and thermoplastics. It is an inexpensive method to attain full-colour prints, but it produces parts with a poor surface finish and their strength is dependent on the adhesive and material used [44].

2.3.7 Vat photo-polymerisation

Photopolymerization encompasses several processes that rely on the same strategy: a liquid photopolymer is contained in a vat, and parts are selectively cured with a heat source. Different curing devices may be used, such as lasers, ultra-violet beams, digital projector screens or even regular LCD screens. Some of the most popular Vat Photo-polymerisation processes include StereoLithograAphy (SLA), Digital Light Processing (DLP), Continuous Liquid Interface Production (CLIP) and Daylight Polymer Printing (DPP). Once again, these processes differ only in copyright, specific implementation, material and curing device. Whereas SLA uses a laser as a curing device, selectively curing points of the print surface and "drawing" the shape of the object layer-by-layer, DLP flashes the entire print surface at once, allowing for much shorter print times, and CLIP uses UV light for curing, with the main innovation being that the process is carried out "from the bottom up", meaning that it is not necessary to wait for the last printed layer to fully cure before continuing the process. DPP uses a regular LCD screen as a curing device, which is only possible due to the use of a specially designed light sensitive resin. Photopolymerization's chief advantages include its high accuracy and quality surface finish, but the parts thus produced tend to suffer from poor mechanical properties, and the material choice is limited (Figure 2.30) [47].

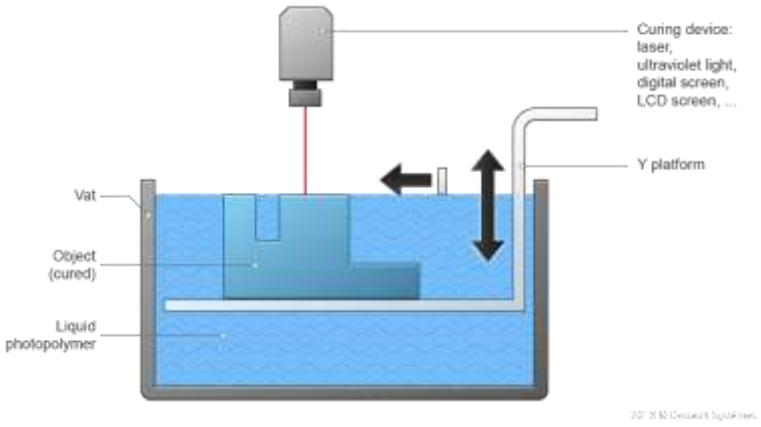

Figure 2.30 - Diagram of Vat Photopolymerization [44]

These categories of additive manufacturing, the materials on which the processes may be applied, their advantages and disadvantages, have been summarised in Table 2.1.

Table 2.1 Categories of Additive Manufacturing, available materials, advantages, and disadvantages

Type	Materials	Advantages	Disadvantages
Binder Jetting	Ceramics Composites Metals Polymers	No support required Inexpensive High Speed Large Build Volume	Poor surface finish Delicate parts
Material Extrusion	Composites Polymers	Multi-material printing Multi-colour printing Fully function parts Inexpensive	Step structed surface Vertical Anisotropy
Directed Energy Deposition	Hybrids Metals	Multiple degrees of freedom of nozzle Higher quality parts	Balance needs to be maintained between speed and finish
Material Jetting	Ceramics Composites Hybrids Polymers	Multi-material printing Smooth surface finish High dimension accuracy	Support required Limited range of material used
Powder Bed Fusion	Ceramics Composites Hybrids Metals Polymers	High speed No support required High accuracy Relatively Inexpensive	Small build size High power consumption Poor surface finish
Sheet Lamination	Ceramics Metals Polymers	Full-colour prints Relatively Inexpensive Ease of material handling Excess material may be recycled	Limited range of material used Poor surface finish Strength depends on adhesive used
Vat photo-polymerisation	Ceramics Polymers	High accuracy High quality surface finish	Limited range of material used Poor mechanical properties

3 Methodologies and design description

The bulk of the practical work itself focused on two different prosthetic devices: a prototype lower-limb active prosthesis developed at BiRDLab, henceforth referred to as the BiRDLab prosthesis, and a smaller model prosthesis to act as a test bed in conjunction with the DARwIn-OP robot, referred to as the DARwIn-OP prosthesis.

3.1 BiRDLab prosthesis

Previous work carried out at the BiRDLab involved the conception and construction of a prototype active foot prosthesis. This prosthesis was based off work carried out at the Massachusetts Institute of Technology, and on the SPARKy prosthesis, a project from the University of Arizona. A new prosthesis was designed making use of a screw and nut to emulate the ankle's motion, and a leaf spring, to provide flexibility and shock absorption, and to correct the axial displacement of the screw (Figure 3.1). The prosthesis' active component is supplied by a small DC motor, which operates a belt and pulley mechanism to rotate the screw. The foot itself would be built out of carbon fibre, combining flexibility and resilience [48].

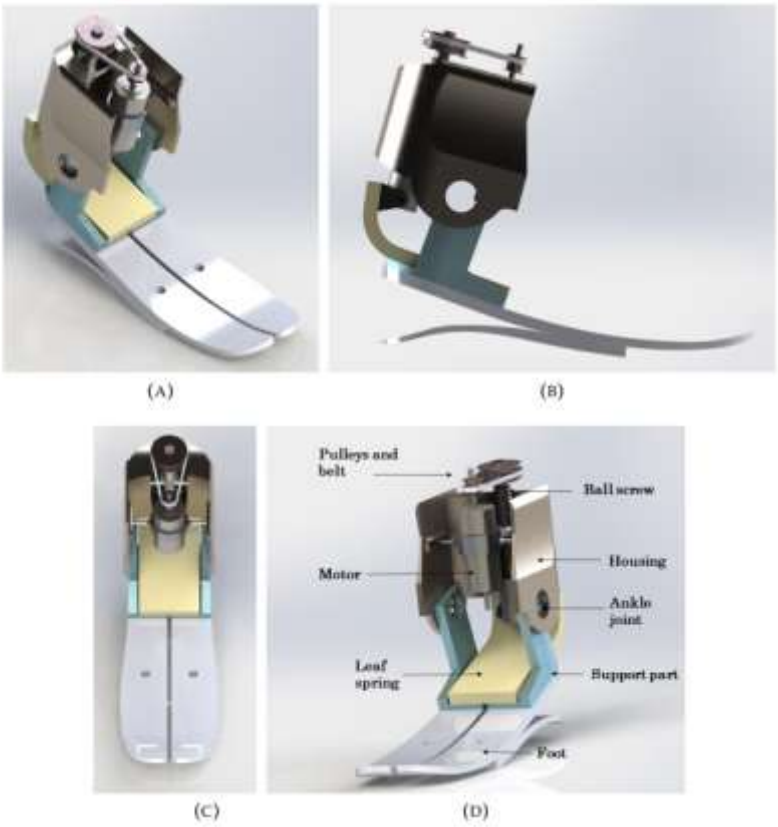

Figure 3.1 - CAD model BiRDLab prosthesis. A), B), C) Different views of the prosthesis. D) Components of the prosthesis [48]

When transitioning from design to implementation, most models and components were redesigned to facilitate machining and assembly. The leaf spring proved to be impossible to acquire economically, and so was replaced by a double pivot, which solves the kinematics of the device, but does not retain the elastic and shock absorption properties of the leaf spring. The carbon fibre foot was graciously provided for free by Össur [48]. The final CAD model and component list is available in Figure 3.2 and the assembled prototype in Figure 3.3.

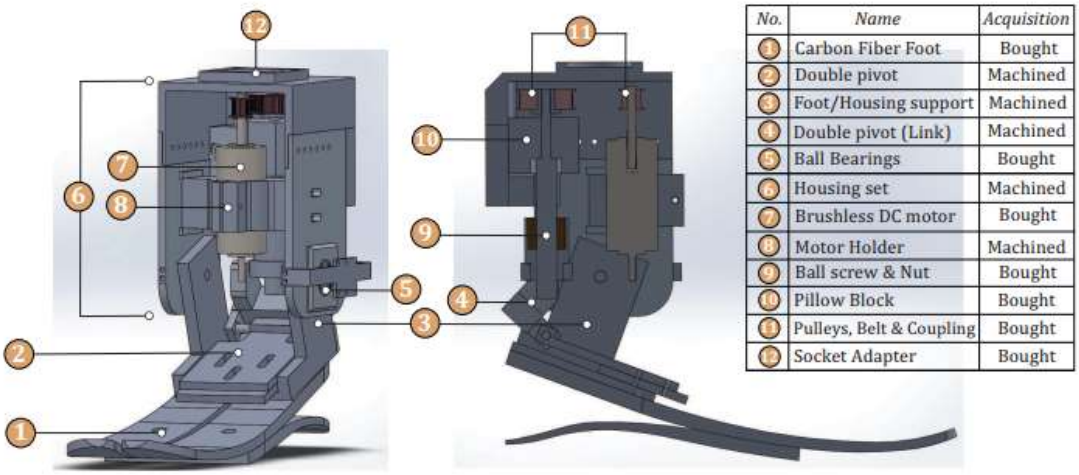

No.	Name	Acquisition
1	Carbon Fiber Foot	Bought
2	Double pivot	Machined
3	Foot/Housing support	Machined
4	Double pivot (Link)	Machined
5	Ball Bearings	Bought
6	Housing set	Machined
7	Brushless DC motor	Bought
8	Motor Holder	Machined
9	Ball screw & Nut	Bought
10	Pillow Block	Bought
11	Pulleys, Belt & Coupling	Bought
12	Socket Adapter	Bought

Figure 3.2 - Final CAD model of BiRDLab prosthesis with components and their sources [48]

Figure 3.3 - Assembled prosthesis and A) Frontal view, B) Rear View, C) With top housing fitted

The prosthesis was correctly assembled and is operational. However, it presents several issues that prohibit its commercialisation. These issues have been summarised in Table 3.1, with a more thorough exploration below.

Table 3.1 - Issues observed in BiRDLab prosthesis and proposed solutions

Observed Issue	Proposed solutions
Excessive weight	Make use of alternative, lighter materials, such as aluminium
	Reduce size of non-critical parts via FEA
	Replace components with 3D Printed alternatives
Low torque at ankle joint	Replacing the motor
	Installation of a reduction drive
	Replacement of the screw by a screw with a smaller lead
	Installation, (and, or) resizing of additional pulleys in the belt transmission
Low energy restoration	Installation of a leaf spring
	Use more flexible materials for the foot
No sensors/control scheme	Installation of sensors using 3D printed brackets
	Implementation of an Arduino-based control scheme

3.1.1 Excessive weight

For a long time, manufacturers have exalted and focused on the importance of the prosthesis achieving the lowest possible weight, which intuitively would lead to a lower energy consumption, thus a more comfortable gait. However, recent studies have shown that it might not be quite as simple and obvious as previously thought. In fact, some studies show no statistically significant impact in energy consumption, while others report a noticeable reduction in energy consumption when using a lighter prosthesis [49], [50]. Further factors that must also be taken into consideration have also been uncovered, such as the fact that a heavier prosthesis will stimulate muscle growth and thus render the user more capable of, and more comfortable with, operating these prostheses. It would seem then that a "weight window" is present, with lighter prostheses leading to muscle atrophy, and heavier prostheses being too heavy to comfortably lift [50]. Some prostheses have a mass of as little as 800g, while others up to 2kg.

It is unfortunately obvious that the BiRD Lab prosthesis fits into the latter category, with an excessive 3.1 kg, without the incorporation of a stronger motor/reductor, batteries, control mechanisms, and others, more than twice the mass of the average sound limb (1.5kg). This is largely due to the use of steel as a material of choice, and the construction of a housing that is oversized in several areas, due to its nature as a quick prototype.

To tackle this excess weight, several strategies are proposed, many of which may be implemented simultaneously. The current prosthesis' housing is made from stainless steel, which may be replaced with aluminium or titanium (albeit financial concerns may also hinder their implementation). More detailed FEA analysis may also permit the shaving off unnecessary material in areas that are not exposed to critical stresses. Finally, 3D printing technologies may also permit the substitution of portions or even the entirety of the housing with ABS or PLA plastics, drastically reducing costs, manufacturing times, and weight.

3.1.2 Low torque at ankle joint

When selecting the motor for the first prototype, the stall torque was wrongfully considered for the selection criteria, thus inducing an error for the motor's torque. The comparison of this value with the required peak torque (around 1Nm) is an inadequate method, as the stall torque of a motor merely indicates the theoretical peak delivered by the motor at zero speed, and not a torque value that the motor can consistently output without overheating or destroying the motor. Nominal torque is a more adequate metric to use, but it may err on the side of caution. Many manufacturers provide information regarding peak torque achievable at a certain percentage of the duty cycle, and further experiments with temperature measurements may be carried out to determine if a proposed motor can provide the required peak torque values for the required points in the gait cycle without suffering from heat or mechanical damage.

The most obvious, but also most expensive solution, is the replacement of the motor by one who fits the requirements. A reduction drive may also be applied to the motor to increase the output torque, as well as tweaking the size of the pulleys that transmit power to the screw, but care must be taken so that the output RPM do not decrease too much, which in turn would lead to the screw not being able to operate fast enough to emulate human gait. Other solutions include the installation of a screw with a smaller lead, and the installation of more pulleys, and the resizing of these.

Calculations were carried out to study whether the required torque could be provided by the motor without compromising the foot's operation. These calculations were only carried out for dorsiflexion, as it is the phase of the human gait with the highest torque requirements (fig. 1.7).

The required torque at the ankle for normal human gait is 1.6Nm/kg, which for a 75kg individual results in 120Nm. Knowing the momentum arm of the ballscrew used in the prosthesis (0.0456m), the force of this screw is calculated as follows:

$$F = \frac{Torque\ at\ ankle\ (120Nm)}{Moment\ Arm\ (0.0456m)} = 2631.58N \tag{5.1}$$

The drive torque, for when rotation is converted to linear motion, is obtained as such:

$$Driving\ Torque = \frac{Axial\ load \cdot Screw\ Lead\ in\ mm}{2 \cdot \pi \cdot \eta\ (efficiency: 90\%)} \cdot 10^{-3} \tag{5.2}$$

$$Driving\ Torque = \frac{2631.58 \cdot 5}{2 \cdot \pi \cdot 0.9} \cdot 10^{-3} = 2.33\ Nm$$

Finally, from the following formula it is possible to know what ratio is required so that motor torque does not exceed the nominal torque provided by the motor's manufacturer (92.9 mNm):

$$Tmotor = \frac{Driving\ Torque \cdot R\ (ratio)}{\eta\ (efficiency: 90\%)} \tag{5.3}$$

$$92.9 \cdot 10^{-3}\ Nm = \frac{2.33 \cdot R}{0.9}$$

$$R = 0.03588 \cong \frac{1}{28}$$

As we can see, to operate within the nominal torque constraints of the motor, the mechanism must impart a 28:1 reduction ratio. We must now calculate whether such a reduction would make it impossible for the ankle joint to keep pace with the gait.

Following the diagram presented in Figure 3.4, which is a simplification of the actuation chain shown in Figure 3.5 we can apply trigonometry to find the maximum vertical displacement during both dorsiflexion (a)(equation 5.4, Xdf) and plantarflexion (b)(equation 5.5, Xpf).

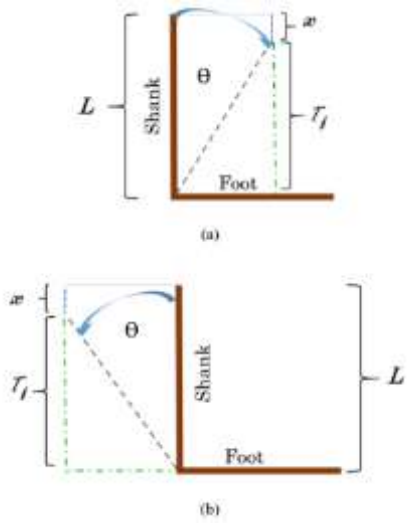

Figure 3.4 - Diagram of prosthesis and important measurements during a) dorsiflexion, and b) plantarflexion

Figure 3.5 - Profile view of the prosthesis' actuation chain

$$Xdf = L(120mm) - Lcos(\theta[10º]) = 1.82mm \quad (5.4)$$

$$Xpf = L(120mm) - Lcos(\theta[25º]) = 11.2mm \quad (5.5)$$

The screw rotational speed is calculated as follows:

$$Nscrew = \frac{LinearVscrew}{Pitch} \quad (5.6)$$

With a screw pitch of 5mm, and a walking speed of 1 stride per 1.2 seconds, the rotational speed of the screw for the stance phase, which represents 62% of the gait and is where dorsiflexion is more present, is calculated by equation 5.7, whereas the screw speed for the swing phase (38% of the gait and dominated by plantarflexion) is calculated by equation 5.8.

$$Nstance = \frac{\frac{1.82mm}{1.2 \cdot 0.62} \cdot \frac{60}{min}}{5mm} = 29.35\ RPM \quad (5.7)$$

$$Nswing = \frac{\frac{11.2mm}{1.2 \cdot 0.38} \cdot \frac{60}{min}}{5mm} = 294.74\ RPM \quad (5.8)$$

These screw speeds must now be translated to motor speed, with the inverse reduction ratio previously calculated, and these values compared to the maximum supplied by the manufacturer (16000 RPM).

$$Nmotor = \frac{N\ screw}{R} \quad (5.9)$$

$$Nmotorstance = \frac{29.35}{\left[\frac{1}{28}\right]} = 821.8\ RPM \quad (5.10)$$

$$Nmotorswing = \frac{297.74}{\left[\frac{1}{28}\right]} = 8336.72\ RPM \quad (5.11)$$

It is therefore concluded that, for a reduction ratio of 28:1, the motor is indeed capable of outputting enough RPM's to properly emulate human gait. Such a large reduction is difficult to achieve with pulleys alone, especially considering the space constraints, so a reduction drive installed in series with the motor seems to be ideal.

3.1.3 Low energy restoration

One of the most important characteristics of the human foot, mainly in the muscular groups, is its ability to reuse some of the energy expended in one cycle of the gait on the next one, which reduces the energy required and increases comfort. Unfortunately, the current prosthesis possesses very little to no energy restoration, merely that which is derived from the natural elasticity of the carbon foot itself. To introduce some energy restoration, it would be adequate to install a leaf spring made from resilient, yet flexible materials, such as Kevlar. Some energy restoration may also be introduced with the employment of more flexible materials in the foot.

3.1.4 No sensors/ no control scheme

The current prosthesis does not include sensors for important information such as position, joint angle, speed, etc. These sensors are crucial to the development of a proper control scheme, so that the prosthesis may operate automatically without the need for user input. Sensors may be easily installed resorting to 3D printed brackets, as these are cheap and perfectly adequate to the low stresses, they are subject to. This sensory information may then be fed into a microcontroller coded with the required control scheme.

Unfortunately, due to budget and facility constraints, plus the ongoing global Covid-19 pandemic, it was not possible to test or implement those proposed solutions. For instance, replacing the housing structure for another one made of a different material and optimized via FEA was too costly, so the possibility of constructing the entirety of the housing out of 3D printed polymers was studied, but also discarded. Further studies, as well as discussions with industry experts, revealed the impossibility of accurately mimicking the physical properties of an object printed through FMD (Fused Deposition Modelling) via software, which would imply that testing would have to be carried out on a trial-and-error basis, thus not viable in the current situation. It was also noted that studies carried out to evaluate the value of 3D printed prosthetic feet highlight the fact that this prosthesis may appear to function, only to suffer from abrupt catastrophic failure in long-term stress tests[51], [52]. While the design of 3D printed prosthesis seems to be adequate, it is concluded that further advances in material and printing techniques are necessary [53]. The Kevlar spring for energy reduction also proved to be too costly, as well as the substitution of the motor and the installation of a reduction drive. The motor manufacturer, Maxon, does not install these in already sold units, so a brand new one with the installed reduction drive would have to be ordered, something which is not financially viable.

3.2 DARwIn-OP Prosthesis

DARwIn-OP (Dynamic Anthropomorphic Robot with Intelligence–Open Platform) (Figure 3.6) is a miniature humanoid-robot platform developed and manufactured by Robotis in collaboration with several universities, such as Virginia Tech and Purdue University. Its main purpose is to assist research in the fields of artificial intelligence, gait algorithms, vision, inverse kinematics, linguistics, among others.

Some of DARwIn-OP's most important specifications include:

- Height: 454.5 mm
- Mass: 2.9 Kg
- Default walking speed: 24 cm/s, 0.25 s/step
- Degrees of Freedom: 20
- Encoders: 3-axis gyro, 3-axis accelerometer, 2 microphones

BiRDLab is in possession of a DARwIn-OP unit for use in research, which was employed throughout this work to test a small foot prosthesis, as seen in Figure 3.7.

Figure 3.6 – DARwIn-OP robot

Figure 3.7 - BiRDLab's DARwIn-OP with fitted foot prosthesis

Before production of the physical prototype of the BiRDLab prosthesis was carried out, a proof-of-concept model was designed at a 70% scale (Figure 3.8) for implementation in the DARwIn-OP, to study the functioning of the mechanism, identify potential issues and test the prosthesis without requiring a test subject. The structural components were printed with FDM, using ABS as material, and assembled with off-the-shelf components, such as the springs, pulleys, and motor, and dubbed as the DARwIn-OP prosthesis. The DARwIn-OP's right foot was removed, as shown in Figure 3.9, and the prosthesis was attached, as seen in Figure 3.10 [1], [48].

Figure 3.8 - CAD model of the DARwIn-OP prosthesis with a) isometric, b) top and c) rear views [1]

Figure 3.9 - DARwIn-OP with right foot removed [1]

Figure 3.10 - DARwIn-OP with attached prosthesis, adapted from [48]

The functioning of the prosthesis is mostly analogous to that of the BiRDLab prosthesis, in a SEA configuration. A brushless DC motor operates a belt and pulley mechanism, which rotates a ballscrew. The main difference is that in the BiRDLab prosthesis the screw operates a pivot that connects to the foot, whereas in the DARwIn prosthesis this ballscrew moves a screw bar up and down, and two springs connect this bar to the heel, inducing dorsiflexion and plantarflexion. A rear view of the prosthesis with labelled components can be seen in Figure 3.11, except for the motor holder and the motor, that sit behind the screw and are visible in a top view on Figure 3.12. A profile view comparing both prosthesis and highlighting important components is available in Figure 3.13.

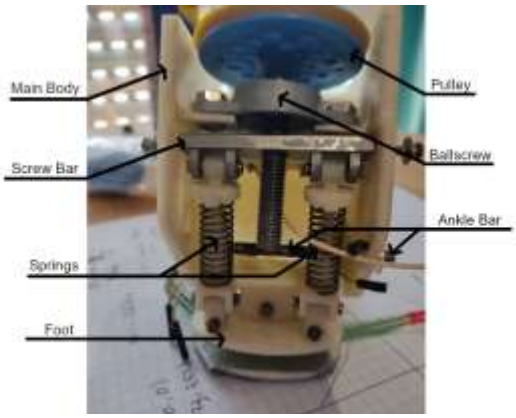

Figure 3.11 - DARwIn-OP prosthesis rear view with labelled components

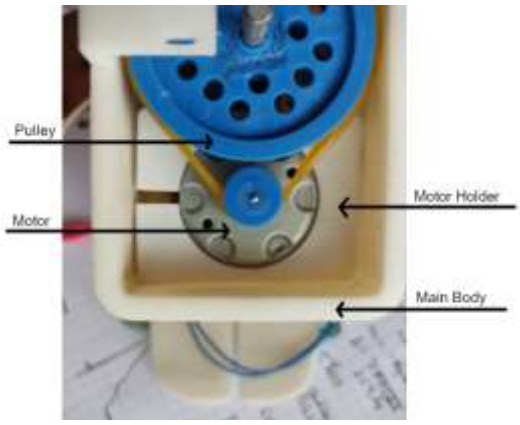

Figure 3.12 - DARwIn-OP prosthesis top view with labelled components

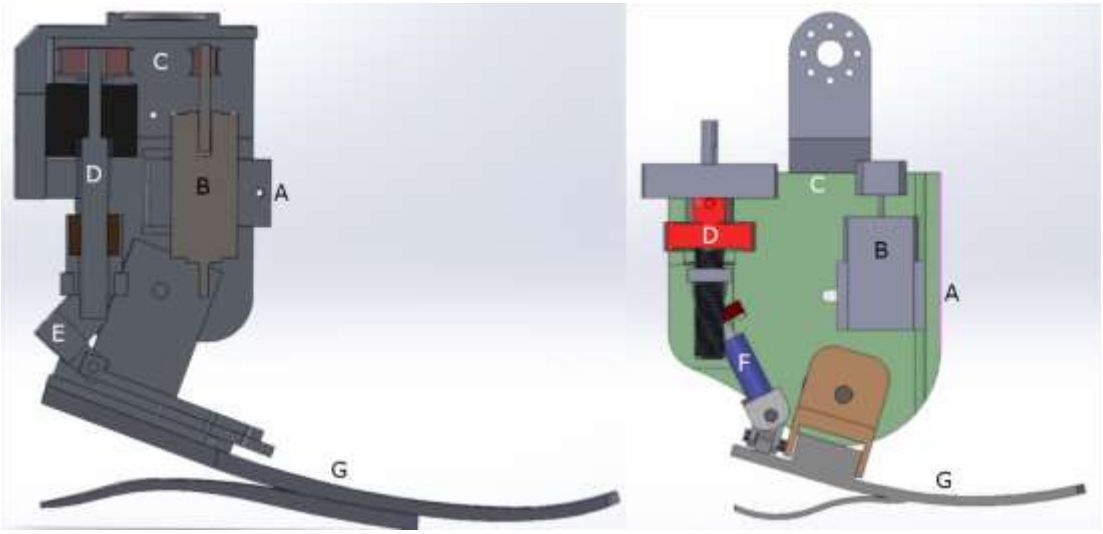

Figure 3.13 - Comparison between the BiRDLab prosthesis (Left) and the DARwIn-OP prosthesis (Right). A) Motor Holder B) Motor C) Pulleys D) Ballscrew E) Double Pivot F) Springs G) Foot

The DARwIn-OP prosthetic foot presented with numerous issues, some of them related to the design of the prosthetic itself, others due to a lack of maintenance. Specifically, the motor was non-functional and was replaced by an unlabelled, salvaged motor, chosen due to its small dimensions, weight, and 12V requirements. Several flimsy tabs had also snapped, namely the ones holding the screw to the main body, and the ones securing the ankle bar in place. These received some temporary quick fixes, until a new part with reinforced structures could be printed from scratch. The motor proved to be incapable of operating the foot with the pre-installed pulleys and belt (which had become stiff and snapped shortly into experimentation), and so a larger pulley and a rubber band were used as a replacement, providing a smooth and functional operation. Another identified design oversight was the excessive weight of the piece securing the motor in place. This piece was made from aluminium and was far stronger than required, and so a 3D printed PLA replacement was fashioned to reduce weight, with two securing screws on each side instead of the previous one, therefore reducing wobble. With these basic maintenance operations carried out, it became possible to conceptualize, design and implement more permanent solutions and improvements (Figure 3.14).

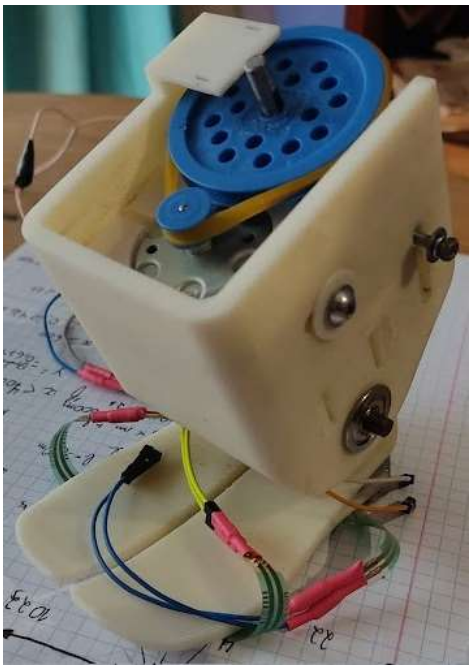

Figure 3.14 - DARwIn-OP Prosthesis after basic maintenance

To operate the prosthesis, a simple code was programmed into an Arduino Uno R3 with a motor shield, which permitted the control of the motor direction and speed via a potentiometer. This code is available in Annex 1 (Figure 3.15).

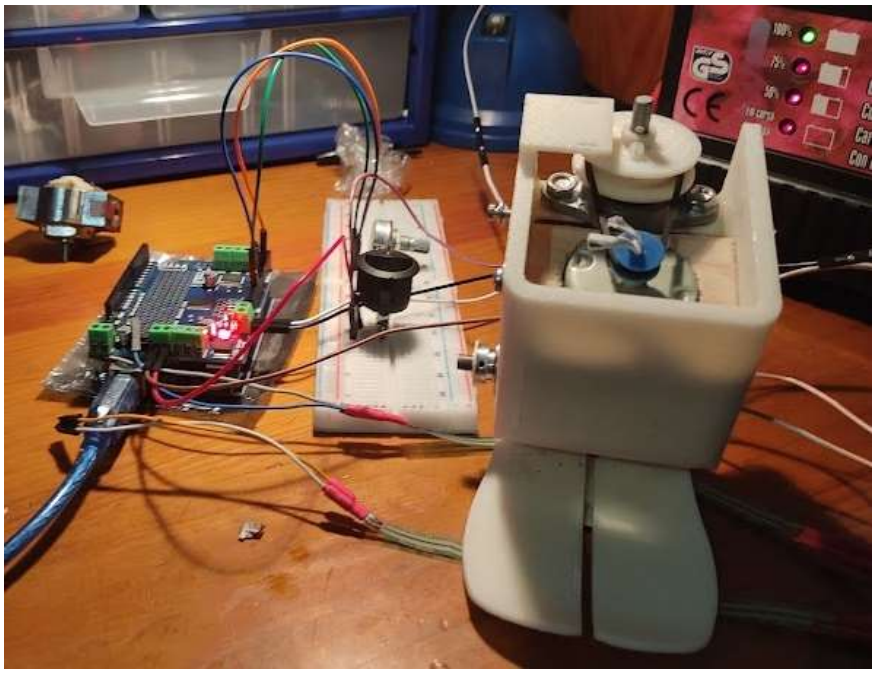

Figure 3.15 - DARwIn-OP Prosthesis and control device

3.2.1 Proposals for DARwIn-OP prosthesis modifications as a case-study for human prostheses.

To improve the function of the DARwIn prosthesis and solve its own issues, as well as function as proof-of-concept tests for the BiRDLab prosthesis, several modifications where proposed and studied. The possibility of using 3D printed structures, more specifically, FDM using PLA, presents a great advantage over tests and prototyping carried out in the original human prosthesis. It permits inexpensive and quick iterations, with new parts and structures being designed, printed, and tested in but a fraction of the time. As such, greater emphasis was placed upon the use of this technology.

3.2.1.1 Planetary Gearing based reduction drive

There are four main types of reduction drives currently available, each presenting with their own advantages and disadvantages. These are planetary gear, worm gear, gear train gear and bevel gear reducers. Planetary gear reducers are compact and light, present virtually no backlash, share power load across all gears (enabling the use of weaker materials like 3D printing polymers), among other advantages. This type of gearbox has a coaxial assembly, making them very compact and thus, ideal for this project. The small dimensions of the DARwIN foot would enable a linear placement of the motor and reducer, but this would be difficult to achieve in the larger human prosthesis due to the much longer motor. A parallel configuration with a belt and pulley transmission would be more easily applicable. While the variation of the size of the pulleys could be used to change the power ratio, the main objective here is to correctly implement a planetary gearset to act as a reduction drive, as a regular pulley transmission cannot achieve the desired ratios in the original prosthesis (Figure 3.16).

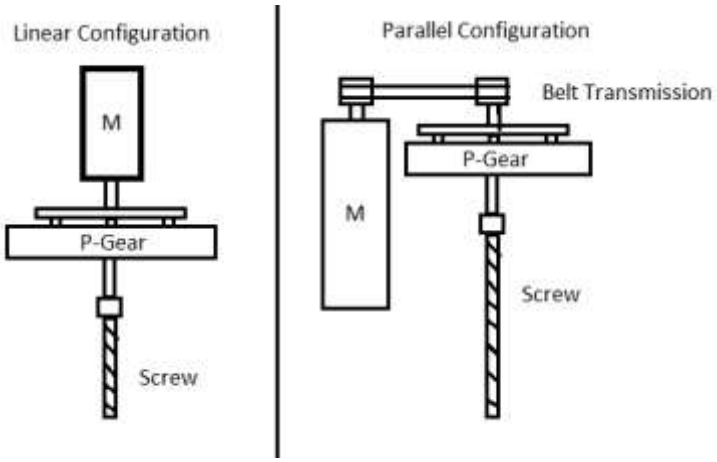

Figure 3.16 - Linear and Parallel configurations for the installation of a planetary gear-based reduction drive

3.2.1.2 Ankle joint axis fixation.

The small flaps that hold the ankle axis in place have snapped. While side to side motion is not a big concern, as the structure of the foot prevents excessive lateral movement, back and forth movement is more dangerous, both in terms of balance as well as damage to the flaps. These should be reinforced and present an opportunity for an elastic shock absorbed to be inserted, which could also contribute to energy restoration. These shock absorbers would take the form of simple rubber blocks, which would be attached to both the small flaps and the foot connector below, as shown in Figure 3.17.

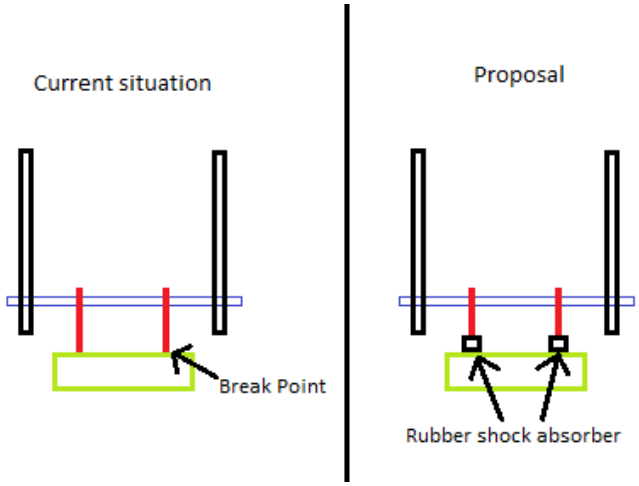

Figure 3.17 - Proposal for reinforcement and improvement of ankle axle fixation flaps

3.2.1.3 Substitution of the motor

Motor included is non-functional and should be replaced. Power and maximum Rpms of substitution motor are not overtly important, as it is not required that the foot be able to operate in real-time for testing purposes. Some of the commercially available motors include the Portescap 16BHS 2-wires, Portescap 22ECT60 Ultra EC or the Maxon EC-max.

3.2.1.4 Testing/adding encoders

Encoders included in the DARwIn-OP foot must be tested, both whether they are operational, accurate, and what metrics are being recorded. Extra encoders such as stretch sensors, pressure sensors and perhaps a temperature sensor on the motor itself may be incorporated.

3.2.1.5 Revised coupling method.

The original method to attach the leg of the DARwIn-OP robot's leg to the prosthesis involved partially disassembling it, as the robot leg fit in between its outer body, and the motor holder, forcing the removal of the latter, which also involves the disassembling of the belt and pulley, and the disassembly of the ankle axle, a very time consuming and impractical method (Figure 3.10, Figure 3.18, Figure 3.19).

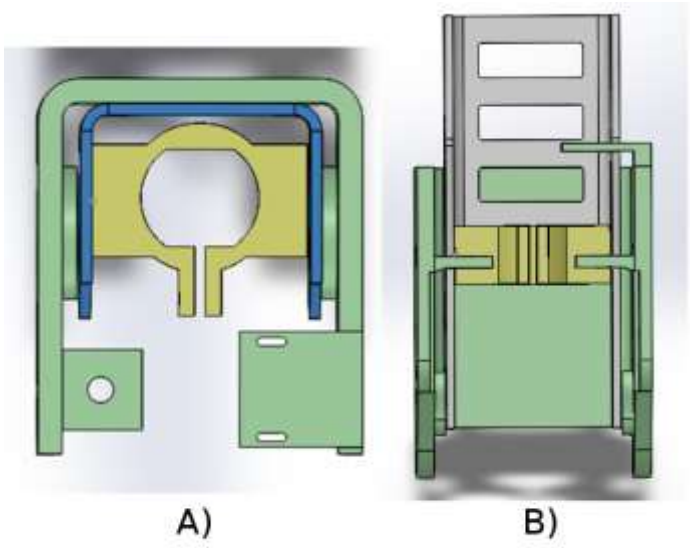

Figure 3.18 - A) Top-down and B) Back-side view of initial attachment method.

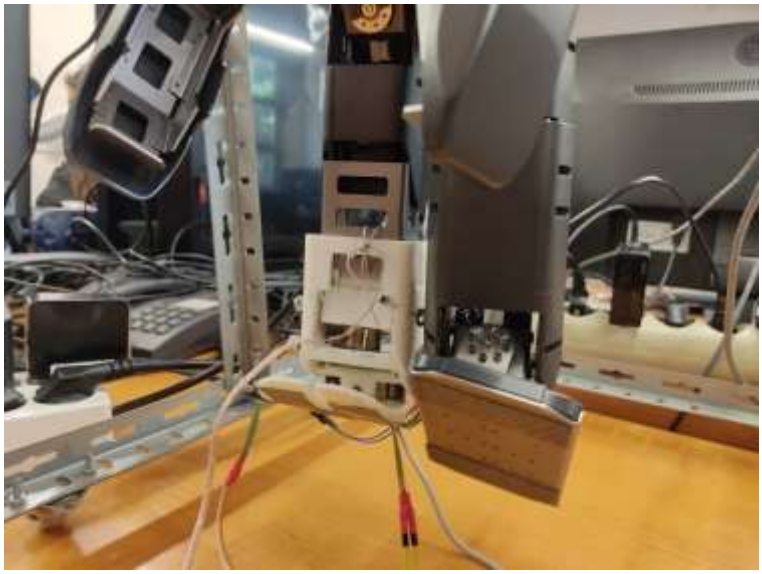

Figure 3.19 - DARwIn-OP with attached prosthesis

Taking inspiration from regular commercially available prostheses (Figure 3.21), a new attachment method was proposed, via the construction of a top piece for the prosthesis capable of holding onto a metallic shaft via either two perpendicular screws, or four lateral screws, as displayed in Figure 3.20. This method would also involve the adaptation of the DARwIn leg so that its lower limit became the metallic shaft. It is also important to note that this adaptation would require careful evaluation and consideration of other factors such as differences in height, balance, and relative position of the leg and foot, to not compromise the robot's ability to walk.

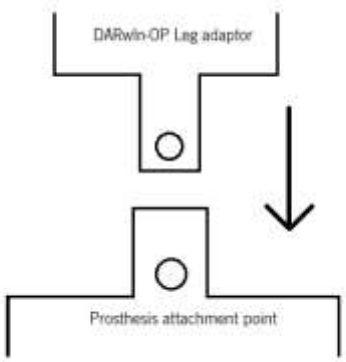

Figure 3.20 - Sketch of proposal for attachment of prosthesis based on linear attachment

Figure 3.21 - Example of commercially available prosthetic attachment port

As an alternative, a simpler attachment method was also proposed, via two structures that can be screwed to the side of the main body and attached directly to the knee of the DARwIn-OP robot (Figure 3.22).

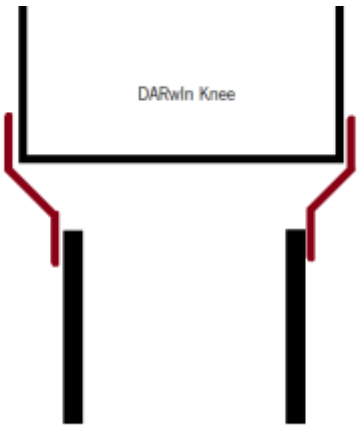

Figure 3.22 - Sketch of proposal for attachment of prosthesis based on lateral attachment points

3.2.1.6 Installation of a timing belt power transmission

The replacement of the belt and pulley transmission from a flat belt into a timing belt transmission is highly beneficial since it will allow better power transmission and less slippage issues. Timing belts are optimal for this application when compared to other types of belts like flat belts, V-belts, or circular belts, since they do not require frequent maintenance and re-tensioning (like V-belts do), or large distances between pulleys (like circular belts do). This modification would also involve the replacement to toothed pulleys, which can be easily designed and manufactured thanks to 3D printing.

3.2.2 Design implementation

These proposals were then evaluated regarding their experimental value, functionality, and viability, and implemented through an iterative process that would constantly take notes regarding any shortcoming or potential improvements. The modifications thus implemented have been categorised regarding what components they affect.

3.2.2.1 Main structure

As previously indicated, the main structure of the prosthesis presented with some wear and tear, and so a new version was printed with a host of improvements. The flaps holding the screw in place, which had snapped in the original body, were thickened from 1.5mm to 3mm, and reshaped to have a wider base, reducing the chances of this same problem occurring again in the future (in orange). A support structure on top of the body meant to fit sensors was removed (in yellow), as it made the changing of the pulleys an extremely inconvenient process that mandated the disassembly of the entire prosthesis. Besides, such a structure can be easily printed and installed via screws afterwards. The lateral holes for the screws that fix the motor holder in position were resized and moved so that the entire motor apparatus can be moved and permit a better alignment of the pulleys (in red). After these changes were designed, a new body was printed in PLA (Figure 3.23 B) to replace the previous one, made of ABS (Figure 3.23 A).

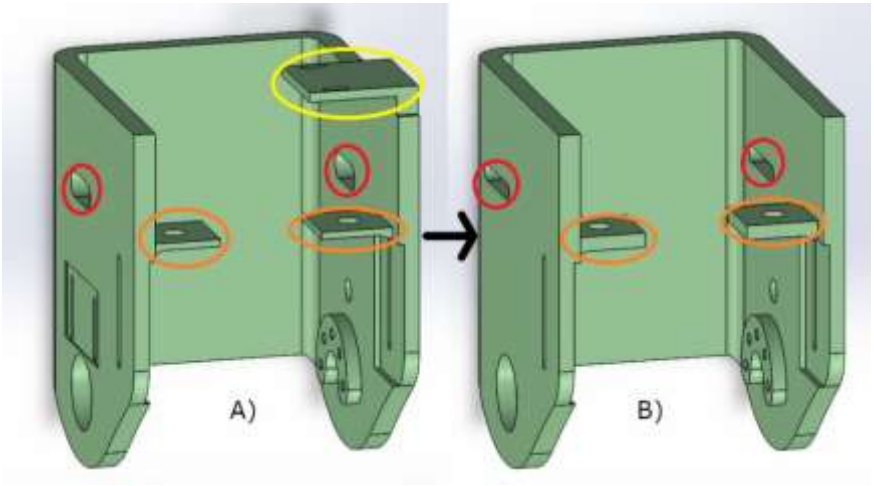

Figure 3.23 - A) Original prothesis' main body, and B) 1st Iteration of prosthesis' main body

Throughout the course of this work, several other modifications were performed to the body, such as cutting a large hole in the front (in green) for the motor holder and for the implementation of a reduction drive (the current design did not allow sufficient space between the pulleys and the belt would not be properly tensioned). It was also necessary to cut new holes for the motor holder screws, placed at a lower height (in blue), as the presence of the reduction drive would cause the associated pulley to be placed too high. Finally, screw-holes for the DARwIn-OP attachment were drilled, as seen in Figure 3.24.

Figure 3.24 - Prosthesis fit with modified main body

The final iteration of the main body was lengthened by 1cm, as spatial constraints had forced the cutting of a front hole, a major structural weakness. A smaller belt was employed, the motor holder screws were once again resized and moved to the appropriate location (in blue), and screw-holes for the attachment mechanism were incorporated in the design. The main body was also widened by 5mm, to better allow the screw bar to slide without getting stuck in the body itself during operation (Figure 3.25).

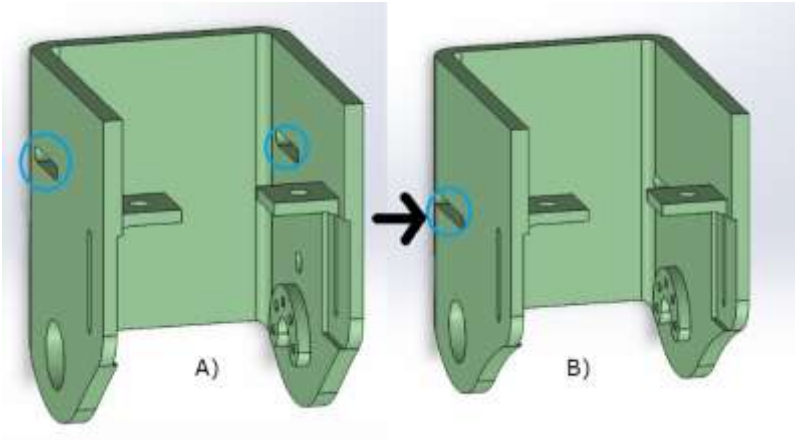

Figure 3.25 - A) 1st Iteration of prosthesis' main body, and B) 2nd and final iteration of prosthesis' main body

3.2.2.2 Motor

The original motor installed in the prosthesis, a Canon DN22 12V, was non-functional, and was substituted by an unlabelled 12V DC motor scavenged off old electronics. Since this motor was not labelled, exact comparison of specifications was not possible. However, it was not a critical issue, as the purpose of the motor was to merely test the mechanisms for their basic functionality, not place them under full load. This motor had the disadvantage of having a wide profile (32mm diameter), mandating a wide motor holder, and hindering its installation within the prosthesis (Figure 3.26).

Figure 3.26 - Salvaged motor with motor holder

This motor was later replaced by a Portescap 22N28 210E.286, a thinner motor (22mm diameter), and whose characteristics are known. Some of the most important are compared in Table 3.2.

Table 3.2 - Comparison of important specifications in two motors

	Canon DN22 M	Portescap 22N28 210E.286	
Voltage	12	12	V
Power	1.3	3.7	W
Stall Torque	10.8	8.6	mNm
Rated Torque	2.45	7.3	mNm
Rated Current	0.19	0.38	A
Max speed	5200	5880	rpm
Weight	40	53	g

We can see that the new motor outperforms the original motor, at the cost of a minimal increase in weight and current draw, and so we conclude that this substitution is more than adequate. The full datasheets are available in the appendices B and C.

3.2.2.3 Motor Holder

The original motor holder, just as in the BiRDLab prosthesis, was made from steel. This material is not ideal, as it results in a piece that is far stronger and heavier than necessary. For such a role, a 3D printed component would be ideal, but as at the beginning of the project a 3D printer hat not yet been acquired, a small motor holder was made from wood. As this was a crude and fast prototype, made to fit the salvaged motor, long term usability was not a concern, and this model lacks the screw holes to tighten the holder around the motor to prevent slippage. The original holder and this wood prototype can be seen in Figure 3.27.

Figure 3.27 - Original metallic motor holder (left) and prototype wood motor holder (right)

As soon as a printer was acquired, a new motor holder was designed and printed. Rather than being fixed to the side of the prosthesis with a single screw on each side, the new holder has two screw holes (3), to prevent the tension from the pulley from spinning the entire motor (2) and its holder on its single axis. Such a change mandated an alteration to the prosthesis' main body, specifically the lengthening of the slots for the screws. Perpendicular to these screws, a mechanism composed by two parallel flaps (1) was designed to permit the tightening of the holder, to better fix the motor in position and prevent slippage (Figure 3.28).

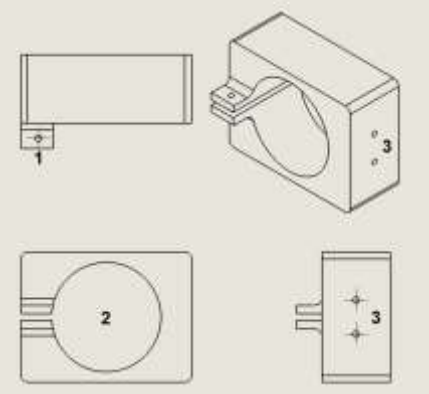

Figure 3.28 - 2D drawing of 1st iteration of motor holder

This first iteration of the motor holder presented some issues. The tightening flaps were too thin and snapped after a few uses, and the screw holes, by virtue of being simple straight holes where the screw would dig its own thread, could not provide adequate grip. As the process of assembling and disassembling the prosthesis during testing wore out the threads, the screws would simply slip. With these issues in mind, a new motor holder was designed, where the tightening screw-hole would be incorporated into the body rather than as two small flaps (1), and where slots for nuts would be included (2). This second iteration is present in Figure 3.29.

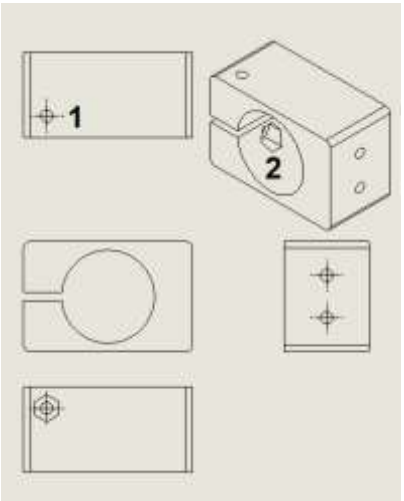

Figure 3.29 - 2D Drawing of 2nd Iteration of motor holder

3.2.2.4 Planetary gear-based reduction drive

The main purpose of a reduction drive is to lower rotational speed and increase torque, and so they are of vital interest for applications such as prostheses, where torque requirements are high, but only relatively little RPM's are necessary to keep pace with human gait. These reduction drives can make use of many arrangements of gears, but of particular interest in this project's context is the planetary arrangement, composed by a central sun gear, an outside ring gear, and intermediary planetary gears that interface between the previous two. This arrangement is compact, permits an easy adjustment of the ratios by altering which gears are driven and which are driving and can achieve gear ratios between 3:1 and 10:1, and so it was decided that it would be interesting to design and implement a 3D printed planetary gear-based reduction drive [54].

A suitable design was found on thingiverse, a website dedicated to the sharing of 3D printed designs. This design (Figure 3.30), created by user "Jtronics", presents as a compact gearbox with the ratio of 4.7:1, and its Creative Commons license enables us to freely modify and publish the design. The only non-printed components in this design are the ball bearings that connect the gears to the carrier piece (3x MR52zz, 1x MR83zz), the gear carrier's axis, and screws.

Figure 3.30 - Assembled 3D printed planetary gear reduction drive by user Jtronics

The original design printed with no issues, but failed to assemble properly, as the gears would not mesh properly, and it proved difficult to insert the planetary gears in the case together with the sun gear. When assembled, the mechanism resisted movement and would often get stuck altogether. Several re-designs and attempts to solve this issue were conducted, from shrinking the gears by a small amount, printing the gears with a brim to avoid the elephants foot effect, re-running the entire printer calibration process to eliminate any minor imperfections in the printing process, among many others.

Later, it was decided to try and print the gears with a different filament, and the issue was immediately resolved. This may be because of the previous filament lower quality or its exposure to ambient moisture causing minute dimension changes, but it just serves to reinforce the importance that the choice of filament has on high-precision prints. Many of the design changes implemented throughout this process were incorporated into the final design. A small brim was implemented in the planetary gears to help hold the bearings in place and the width of these gears was increased (to minimize the tilting of the axis caused by the tension from the belt on the pulley) (Figure 3.31). A covered gear top was for the central gear was designed, to impede the infiltration of lubricant that would cause the motor's axis to fail to grip the sun gear properly, and the replacement of the metal axis with a 3D printed one incorporated into the gear carrier itself (Figure 3.32).

Figure 3.31 - Original planetary gear (Left) and redesigned planetary gear (Right)

Figure 3.32 - Planetary gear carrier with incorporated axis

3.2.2.5 Pulleys

The pulleys in this timing belt drive act as the interface between the axles on both the reduction drive and the main screw, and the belt responsible for transmitting power between these. They are also capable of acting as reduction drives, depending on the relative sizes of the pulleys, with the ratio given by the simple formula:

$$Ratio = \frac{nº\ Teeth\ Driven\ Pulley}{nº\ Teeth\ Drive\ Pulley} \tag{5.12}$$

The original pulleys in the prosthesis were designed to accommodate a flat belt, and so had to be replaced when the decision was made to switch to a toothed belt, and especially after the original flat belt snapped and all replacements proved too wide for the old pulleys.

Just as with the reduction drive, a suitable open-source design was discovered on thingiverse, a parametric design by user "droftarts", which allows users to alter several parameters quickly and easily, such as the profile of the pulley, the number of teeth, the presence and size of a retainer, among others. This design served as the basis for the design and printing of two pulleys following the GT2 profile, the same as the toothed belt. To maximize the reduction ratio and to provide yet more torque, the drive pulley was designed to be as small as possible without compromising its structural integrity, while complying with the dimensions required by the GT2 profile, coming out

at a total of 14 teeth (Figure 3.33 A). The size of the driven pulley was determined as a function of the size of the belt (158mm), and the maximum diameter allowed for this pulley by the main body of the prosthesis (circa 50mm). Care was taken to ensure that it is possible to install and tense the belt slightly without damaging the plastic axis of the reduction drive, and that the components do not collide with each other or with the body of the prosthesis, resulting in a driven pulley with 63 teeth, for a total reduction ratio of 4.5:1 (Figure 3.33 B).

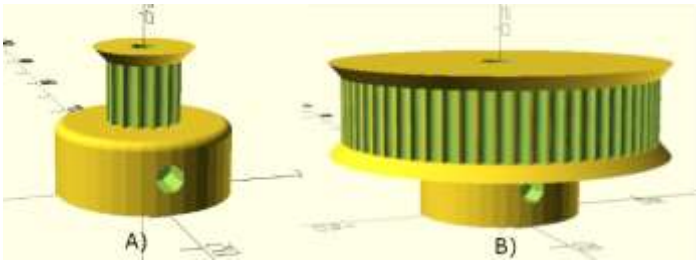

Figure 3.33 - A) Drive pulley and B) Driven pulley.

3.2.2.6 Belt

The belt that had been used in previous work with the prosthesis was a flat, thin belt which snapped shortly into experimentation, and had to be replaced. Until a new belt could be sourced, experiments were carried out resorting to a rubber band, which proved to be unsuitable, suffering from excessive slippage. It was decided that its replacement would be a timing belt (also known as toothed belt, or synchronous belt), which are more suited to transmit high levels of torque and prevent slipping, with some of the downsides being the necessity of specific pulleys and being more expensive than traditional flat belts [55].

Several sizes were experimented with, but it was ultimately decided to use a GT-2 type, 158mm length and 6mm width belt (Figure 3.34), which proved to be an adequate size to permit the installation of the pulleys within the size constraints presented by the main body of the prosthesis. Larger belts would necessitate either a lengthening of the main body itself, or the re-sizing of the pulleys to such a degree where they would become wider than the body and would have to be installed above it. Shorter belts could be used, but they would necessitate the downsizing of the driven pulley, decreasing its reduction ratio. The specific size of the belt, 158mm, was determined to be the best fit from among the supplier's offer, which included sizes such as 122mm, 200mm, 280mm, among others.

Figure 3.34 - 158mm GT2 Toothed Belt.

3.2.2.7 Assembly method

As discussed previously, the mechanism to attach the prosthesis to the DARwIN-OP Robot proved inadequate and laborious, as attaching, or detaching the prosthesis involved its almost complete disassembly, and the tightening and loosening of screws in awkward positions and tight spaces (Fig.4.5). It was then decided to develop a revised and simplified method, in which two lateral flaps would connect directly to the DARwIN-OP's knee joint, rather than its leg connecting to the ankle of the prosthesis, as per sketched in Figure 3.22.

The first iteration of this revised component consisted of two structures that would sit on top of the prosthesis' own body, be fixed in place via two screws, and connected via a horizontal bar, to mimic DARwIN's own leg structure (Figure 3.35, Figure 3.36). Due to miscalculations in the distance of this horizontal bar and the knee itself, and an unexpected fast and total extension of the knee during testing, the bar impacted the knee and snapped, leaving the two vertical structures with no connection. However, further testing did demonstrate that such a horizontal connector was wholly unnecessary, and that the movement of the join was not affected by the omission of this component.

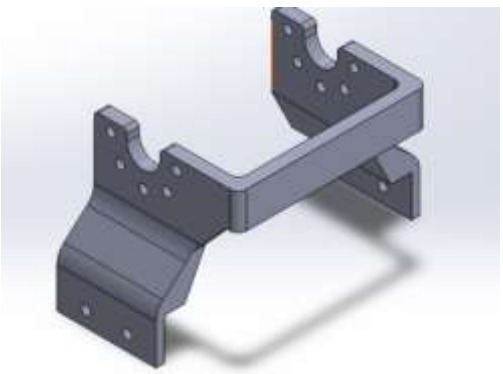

Figure 3.35 - First iteration of the prosthesis-knee attachment component

Figure 3.36 - First iteration of the attachment component connected to DARwIN-OP's knee

As such a second iteration of this component was designed, removing the unnecessary horizontal bar, increasing the height of the lateral pieces by 5mm, and providing the complete circular structure for attachment to the knee joint (as opposed to the previous semi-circle) (Figure 3.37, Figure 3.38).This separation of the lateral supports into separate pieces also provides the advantage that, in event of further damage, it is possible to replace one of the pieces without also replacing the other.

Figure 3.37 - Second iteration of the prosthesis-knee attachment component

Figure 3.38 - DARwIn prosthesis attached with revised attachment method

4 Results and Discussion

As previously discussed, budget and facility constraints, as well as other events, such as the COVID-19 pandemic, prohibited the implementation and testing of modifications to the BiRDLab prosthesis, but valuable information for any future works was attained regardless, specifically regarding the use of additive manufacturing in the production of the prosthesis.

While Additive Manufacturing techniques have improved a lot since their earlier days, there remain concerns regarding strength, durability, and consistency of the parts acquired in this fashion. There appear to be no tools or software suites capable of accurately simulating the properties of these structures, largely due to their layered construction (in the case of FDM and others), and minute differences between the layers. Therefore, the only viable way to test these components is via experimental procedures, but even these are of dubious quality since the properties of the printed components can vary a lot between components due to several factors, such as air moisture and temperature at the time of the printing, the quality and consistency of the material, the specific parameters of resolution, printing speed, temperatures, among others. Further technological developments in both simulation software and manufacturing techniques capable of greater consistency would therefore be of great interest to several industries, including the prosthetic market. As it stands, it seems that materials printed with FDM techniques may be adequate for external coverings and internal component holders, but not for the load bearing structures themselves.

It was also possible to confirm the issues that the prosthesis suffers, from excessive weight to an underpowered motor, among others, and theorize several solutions to these issues. The calculations to obtain the necessary reduction ratio for the currently installed motor to be able to operate the mechanism properly were also performed.

More practical work was carried out on the DARwIn-OP prosthesis, due to its smaller nature that permitted the use of more affordable FDM and off-the-shelf components. An iterative process identified flaws with the original design, such as poor maintenance and shortcomings with the design of the main structure that rendered the prosthesis inconvenient to instal and operate. These shortcomings were then corrected, resulting in the final version of the prosthesis, with a new main body, a new motor holder, an FDM-printed planetary gear reductor, new pulleys and belt, and a new, more convenient, attachment component to interface with the DARwIn-OP's knee. A control

device was implemented with an Arduino R3 board that permits the permits the operation of the motor with a potentiometer, and the prosthesis was attached to the DARwIn-OP for testing, as can be observed in Figure 4.1.

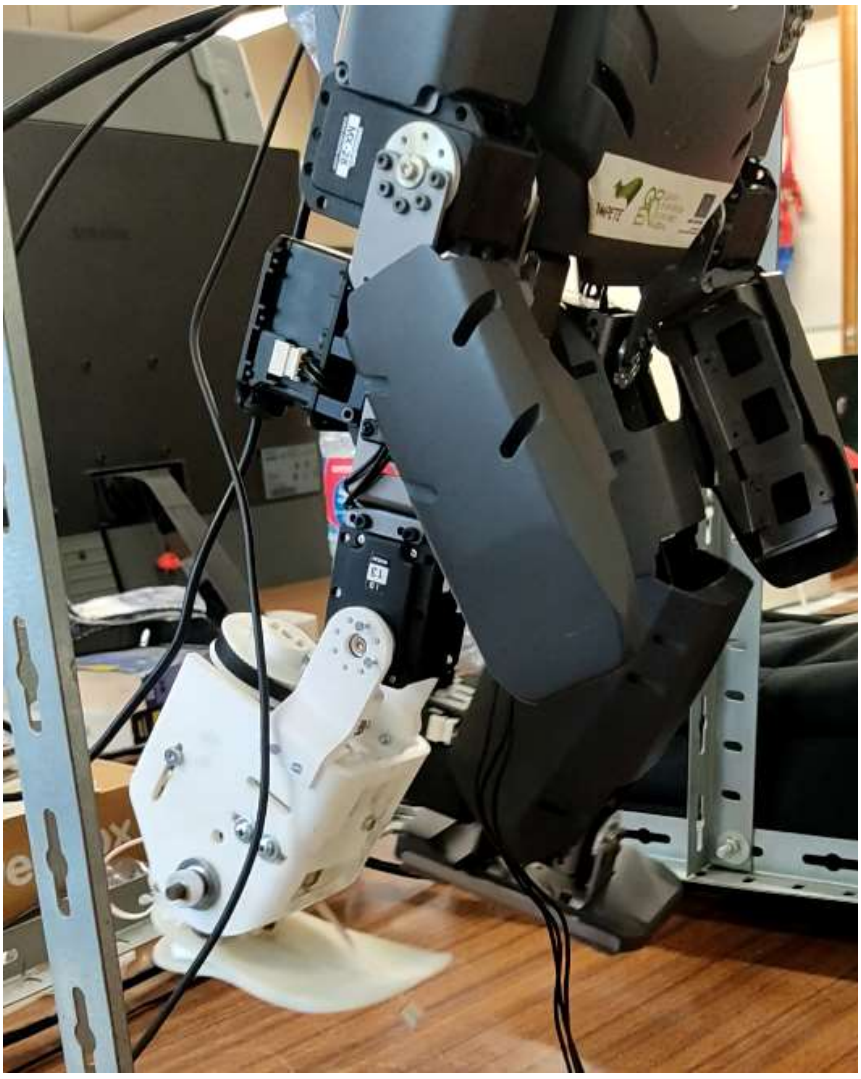

Figure 4.1 - DARwIn-OP with fitted prosthesis, in hanging harness

Before any work regarding the integration of the active movement of the prosthesis with the DARwIn-OP's gait was carried out, it was decided to test the functionality of the prosthesis as a purely passive device. Due to the differences in size and kinematics of the prosthesis and the original foot, modified code allowing for the independent and modifiable movement of the right leg and foot was implemented, and the DARwIn was set on a flat surface. It was observed that it proved capable of remaining upright, so long as it didn't move, as per Figure 4.2.

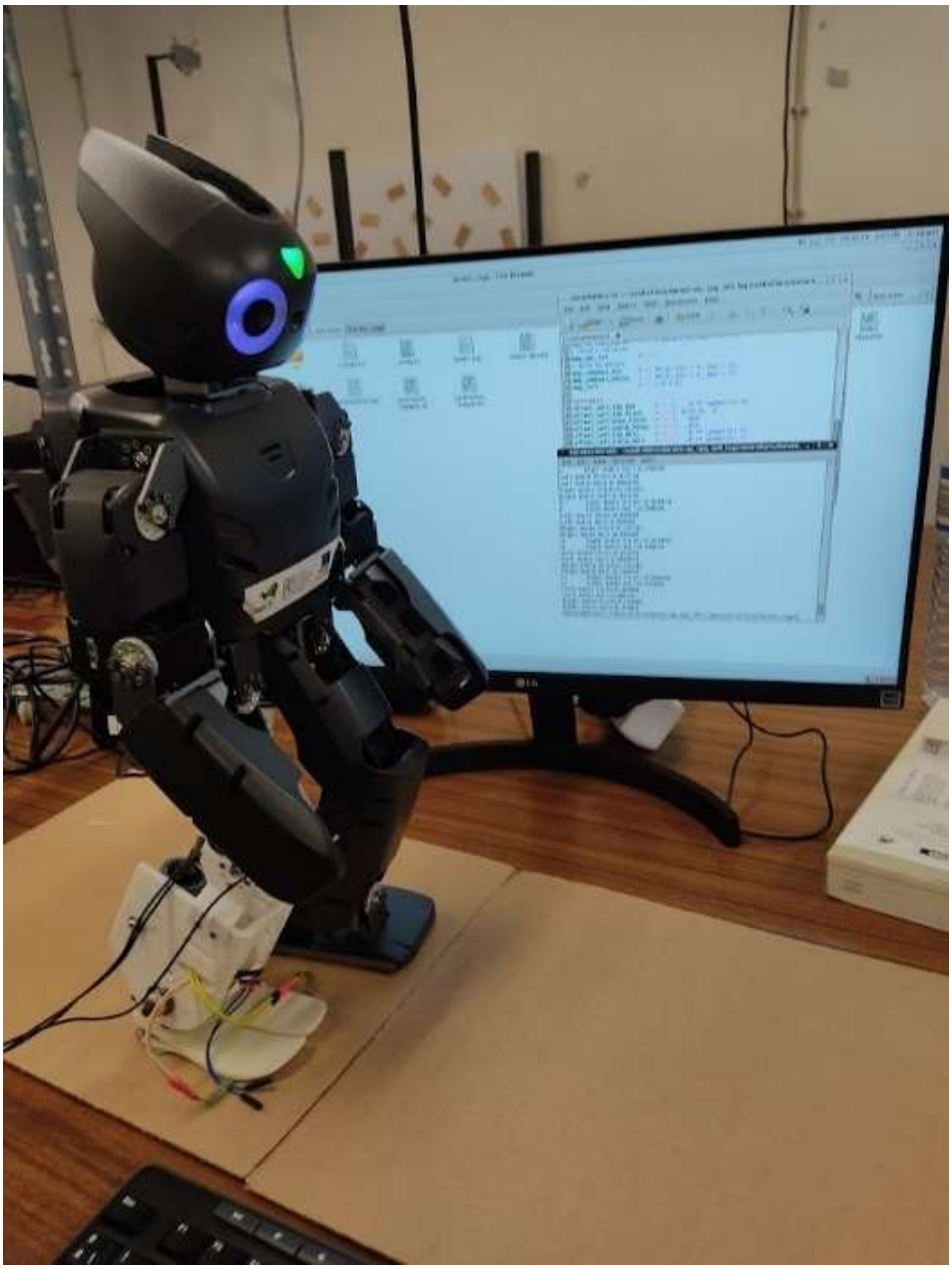

Figure 4.2 - DARwIn-OP standing upright with fitted prosthesis

When the command to initiate movement was given, the results were less positive, and the DARwIn proved to be incapable of staying upright. As it shifted its weight to the prosthesis, to initiate the swing phase of the healthy limb, the springs of the prosthesis would compress, "sinking" the limb closer to the walking surface, making it so that the healthy limb never left the ground before the code initiated the swing phase, violently throwing the robot backwards. Other issues were observed, such as an incorrect angle in the knee joint of the prosthetic limb, and no compensation on the healthy limb, as this had not yet been programmed. Despite multiple attempts to alter the parameters of the walking code based on visual feedback and attempts at reducing the elasticity of the prosthesis with rubber blocks, proper gait could not be established without a human holding up and balancing the DARwIn, as can be seen in Figure 4.3.

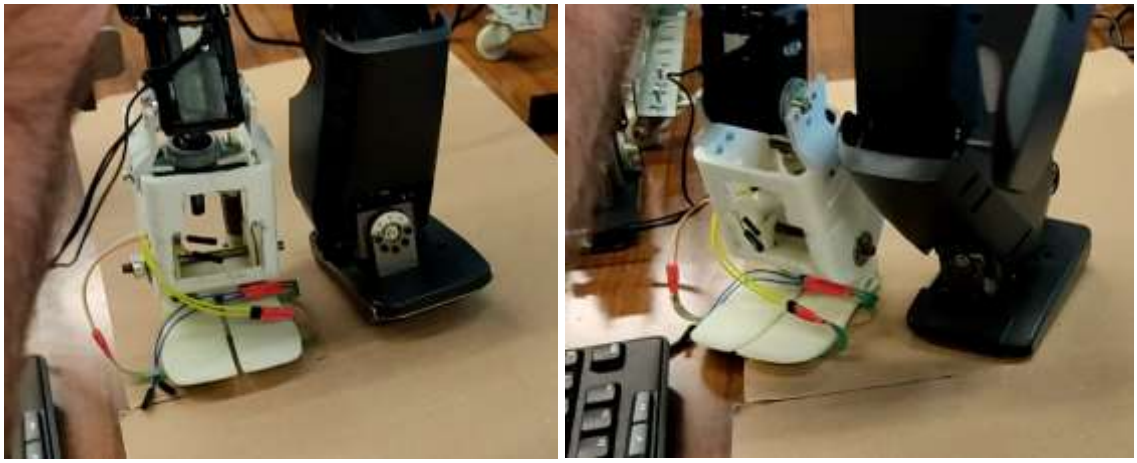

Figure 4.3 - DARwIn-OP with fitted prosthesis struggling to maintain balance

As such, it is now possible to provide answers to the research questions posed previously:

- Is it possible to develop an affordable and functional prototype active lower-limb prosthesis for further testing with patients without access to expansive and expensive facilities and personnel?

Further work is required. While additive manufacturing presents a clear opportunity for cost reduction, it was only successfully applied to a model prosthesis, so testing must be carried out to verify if the proof-of-concept modifications can be applied to the larger prosthesis.

- Can additive manufacturing techniques be employed to reduce the cost and time required to build and iterate prosthesis prototypes?

Yes. Throughout this work, several iterations of various components were quickly designed, printed, and installed at a fraction of the cost and time that it would take more traditional manufacturing and prototyping techniques.

- Can additive manufacturing techniques produce components that have functional roles in prosthesis, or merely for aesthetic coverings and prototyping work?

Yes. In this work, several functional components were successfully designed, printed, installed, and tested successfully, among them a planetary gear-based reductor, which is an otherwise expensive and proprietary component.

- Can proof-of-concept work carried out in small bipedal robots be translated to innovations in the design and construction of prosthesis for human patients?

Further work is required. While the work in the small model prosthesis provided new concepts and ideas for implementation in the prosthesis itself, these must be implemented and tested before conclusions can be drawn.

5 Conclusions and future work

A state-of-the-art review was carried out regarding the prosthetic industry, the human gait, and the effects than an amputation has on it and on additive manufacturing techniques. An analysis was carried out on a prototype active lower-limb prosthesis, to identify potential issues and suggest modifications to alleviate said issues and improve functionality. As a test bed, a similar process of analysis was carried out on a model prosthesis designed to fit a DARwIn-OP robot, and the modifications were implemented and tested.

The modifications implemented in this smaller prosthesis include those brought on by basic maintenance and other adjustments for convenience's sake, but also the installation of a novel motor holder, a planetary gear-based reductor produced with additive manufacturing techniques (FDM in specific), a new system of pulleys with a timing belt and a new, more convenient attachment method. This modified prosthesis was installed successfully on the DARwIn-OP, and it was found to maintain balance while in a stationary position. It was not possible to achieve balanced gait with the prosthesis, nor the integration of the control mechanisms of the active components of the prosthesis with those of the DARwIn, but many opportunities for future work were also laid out.

Regarding the BiRDLab prosthesis, future work could focus on the installation of the proposed modifications, such as including a reductor, construction of a main body with different materials, including stronger additive manufacturing materials, such as PETG, and the testing and iteration of these modifications, culminating in tests with patients.

Regarding the DARwIn-OP prosthesis, future work should focus on adjusting the gait parameters and, if necessary, the prosthesis itself to achieve passive functionality at a minimum, and later, via the integration of encoders with the control mechanisms, full active functionality capable of providing energy at the requisite moments of the gait cycle. Simulation software, such as gazebo, may prove indispensable in solving the kinematics of the prosthesis and arriving at the correct parameters and adjustments to the gait itself.

References

[1] J. Alves, "Dynamic Model of a Transtibial prosthesis," Guimarães, 2016.

[2] R. A. Agha, H. Muneer, and A. AlQaseer, "Major Lower Limb Amputation : Causes, Characteristics and Complications," *Bahrain Med. Bull.*, vol. 39, pp. 159–161, 2017.

[3] L. Ferreira, A. Carvalho, and R. Carvalho, "Short-term predictors of amputation in patients with diabetic foot ulcers.," *Diabetes Metab. Syndr.*, vol. 12, no. 6, pp. 875–879, Nov. 2018, doi: 10.1016/j.dsx.2018.05.007.

[4] Observatório Nacional da Diabetes, "Diabetes: factos e números, o ano de 2015," 2016.

[5] I. Machado Vaz, V. Roque, S. Pimentel, A. Rocha, and H. Duro, "Psychosocial Characterization of a Portuguese Lower Limb Amputee Population," *Acta Médica Port. Vol 25, No 2 March-AprilDO - 10.20344/amp.27* , [Online]. Available: https://actamedicaportuguesa.com/revista/index.php/amp/article/view/27.

[6] K. R. Sellegren, "An Early History of Lower Limb Amputations and Prostheses.," *The Iowa Orthopaedic Journal*, vol. 2. pp. 13–27, 1982.

[7] R. Versluys, P. Beyl, M. Van Damme, A. Desomer, R. Van Ham, and D. Lefeber, "Prosthetic feet: State-of-the-art review and the importance of mimicking human anklefoot biomechanics," *Disability and Rehabilitation: Assistive Technology*, vol. 4, no. 2. pp. 65–75, 2009, doi: 10.1080/17483100802715092.

[8] N. E. Akalan and S. Angin, "Chapter 29 - Kinesiology of the human gait," S. Angin and I. E. B. T.-C. K. of the H. B. Şimşek, Eds. Academic Press, 2020, pp. 499–525.

[9] M. Silva, E. F. Shepherd, W. O. Jackson, F. J. Dorey, and T. P. Schmalzried, "Average patient walking activity approaches 2 million cycles per year: Pedometers under-record walking activity," *J. Arthroplasty*, vol. 17, no. 6, pp. 693–697, 2002, doi: https://doi.org/10.1054/arth.2002.32699.

[10] C. L. Vaughan, B. L. Davis, and J. C. O'Connor, *Dynamics of Human Gait*, 2nd ed. Cape Town: Kiboho Publishers, 1992.

[11] C. L. Brockett and G. J. Chapman, "Biomechanics of the ankle," *Orthop. Trauma*, vol. 30, no. 3, pp. 232–238, Jun. 2016, doi: 10.1016/j.mporth.2016.04.015.

[12] N. S. I. Clinic, "What is Pronation? Is Pronation normal?," 2017. https://www.newcastlesportsinjury.co.uk/what-is-pronation-is-pronation-normal/ (accessed Nov. 15, 2020).

[13] C. S. Moriguchi, T. O. Sato, and H. J. C. Gil Coury, "Ankle movements during normal gait evaluated by flexible electrogoniometer," *Brazilian J. Phys. Ther.*, vol. 11, pp. 205–211, 2007, [Online]. Available: http://www.scielo.br/scielo.php?script=sci_arttext&pid=S1413-35552007000300006&nrm=iso.

[14] R. Donatelli, "Normal Biomechanics of the Foot and Ankle," *J. Orthop. Sport. Phys. Ther.*, vol. 7, no. 3, pp. 91–95, Nov. 1985, doi: 10.2519/jospt.1985.7.3.91.

[15] K. Hollander and T. Sugar, "Powered Human Gait Assistance," in *Rehabilitation Robotics*, 2007, pp. 203–220.

[16] J. Perry and J. M. Burnfield, Eds., "Gait Analysis: Normal and Pathological Function," *J. Sports Sci. Med.*, vol. 9, no. 2, p. 353, Jun. 2010, [Online]. Available:

https://www.ncbi.nlm.nih.gov/pmc/articles/PMC3761742/.

[17] E. Isakov, O. Keren, and N. Benjuya, “Trans-tibial amputee gait: time-distance parameters and EMG activity.,” *Prosthet. Orthot. Int.*, vol. 24, no. 3, pp. 216–220, Dec. 2000, doi: 10.1080/03093640008726550.

[18] B. S. Baum, H. Hobara, K. Koh, H. J. Kwon, R. H. Miller, and J. K. Shim, “Amputee Locomotion: Joint Moment Adaptations to Running Speed Using Running-Specific Prostheses after Unilateral Transtibial Amputation.,” *Am. J. Phys. Med. Rehabil.*, vol. 98, no. 3, pp. 182–190, Mar. 2019, doi: 10.1097/PHM.0000000000000905.

[19] J. Gane, “Running - Blade XT vs Standard Prosthetic Foot,” 2018. .

[20] F. A. de Laat, G. M. Rommers, P. U. Dijkstra, J. H. Geertzen, and L. D. Roorda, “Climbing stairs after outpatient rehabilitation for a lower-limb amputation.,” *Arch. Phys. Med. Rehabil.*, vol. 94, no. 8, pp. 1573–1579, Aug. 2013, doi: 10.1016/j.apmr.2013.01.020.

[21] S. M. H. J. Jaegers, J. H. Arendzen, and H. J. de Jongh, “Prosthetic gait of unilateral transfemoral amputees: A kinematic study,” *Arch. Phys. Med. Rehabil.*, vol. 76, no. 8, pp. 736–743, 1995, doi: https://doi.org/10.1016/S0003-9993(95)80528-1.

[22] V. J. Harandi *et al.*, “Gait compensatory mechanisms in unilateral transfemoral amputees,” *Med. Eng. Phys.*, vol. 77, pp. 95–106, 2020, doi: https://doi.org/10.1016/j.medengphy.2019.11.006.

[23] T. van der Stockt, “Prosthethic Feet,” *Physiopedia*. https://www.physio-pedia.com/Prosthetic_Feet (accessed May 31, 2021).

[24] M. Lusardi and C. Nielson, “Prosthetic feet,” *Orthotics and Prosthetics in Rehabilitation*, 2007. https://www.amputee-coalition.org/resources/prosthetic-feet/ (accessed May 31, 2021).

[25] M. R. Menard and D. Murray, “Subjective and Objective Analysis of an Energy-Storing Prosthetic Foot,” *JPO J. Prosthetics Orthot.*, vol. 1, pp. 220–230, 1989.

[26] J. M. Casillas, V. Dulieu, M. Cohen, I. Marcer, and J. P. Didier, “Bioenergetic comparison of a new energy-storing foot and SACH foot in traumatic below-knee vascular amputations.,” *Arch. Phys. Med. Rehabil.*, vol. 76, no. 1, pp. 39–44, Jan. 1995, doi: 10.1016/s0003-9993(95)80040-9.

[27] P. Lenka and R. Kumar, “Gait Comparisons of Trans Tibial Amputees with Six Different Prosthetic Feet in Developing Countries,” *Indian J. Phys. Med. Rehabil.*, 2010.

[28] B. Verrelst, R. Van Ham, B. Vanderborght, D. Lefeber, F. Daerden, and M. Van Damme, “Second generation pleated pneumatic artificial muscle and its robotic applications,” *Adv. Robot.*, vol. 20, no. 7, pp. 783–805, Jan. 2006, doi: 10.1163/156855306777681357.

[29] H. Zheng and X. Shen, “Design and Control of a Pneumatically Actuated Transtibial Prosthesis,” *J. Bionic Eng.*, vol. 12, no. 2, pp. 217–226, 2015, doi: https://doi.org/10.1016/S1672-6529(14)60114-1.

[30] K. B. Fite, T. J. Withrow, K. W. Wait, and M. Goldfarb, “A Gas-Actuated Anthropomorphic Transhumeral Prosthesis,” in *Proceedings 2007 IEEE International Conference on Robotics and Automation*, 2007, pp. 3748–3754, doi: 10.1109/ROBOT.2007.364053.

[31] P. Cherelle, G. Mathijssen, Q. Wang, B. Vanderborght, and D. Lefeber, “Advances in Propulsive Bionic Feet and Their Actuation Principles,” *Adv. Mech. Eng.*, vol. 6, p. 984046,

Jan. 2014, doi: 10.1155/2014/984046.

[32] M. Grimmer and A. Seyfarth, "Stiffness adjustment of a Series Elastic Actuator in an ankle-foot prosthesis for walking and running: The trade-off between energy and peak power optimization," *2011 IEEE Int. Conf. Robot. Autom.*, pp. 1439–1444, 2011.

[33] D. Rodriguez-Cianca *et al.*, "A Variable Stiffness Actuator Module With Favorable Mass Distribution for a Bio-inspired Biped Robot," *Front. Neurorobot.*, vol. 13, p. 20, 2019, doi: 10.3389/fnbot.2019.00020.

[34] P. Cherelle, V. Grosu, M. Cestari, B. Vanderborght, and D. Lefeber, "The AMP-Foot 3, new generation propulsive prosthetic feet with explosive motion characteristics: design and validation," *Biomed. Eng. Online*, vol. 15, no. 3, p. 145, 2016, doi: 10.1186/s12938-016-0285-8.

[35] Q. Wang, K. Yuan, J. Zhu, and L. Wang, "Walk the Walk: A Lightweight Active Transtibial Prosthesis," *IEEE Robot. Autom. Mag.*, vol. 22, no. 4, pp. 80–89, 2015, doi: 10.1109/MRA.2015.2408791.

[36] R. Bellman, M. Holgate, and T. Sugar, *SPARKy 3: Design of an active robotic ankle prosthesis with two actuated degrees of freedom using regenerative kinetics*. 2008.

[37] BionX, "BionX emPOWER Prosthetic," *MantaDesign*. https://mantadesign.com/work-robotic-prosthetic-design-engineering/ (accessed Sep. 10, 2021).

[38] C. Comotti, D. Regazzoni, C. Rizzi, and A. Vitali, "Additive Manufacturing to Advance Functional Design: An Application in the Medical Field," *J. Comput. Inf. Sci. Eng.*, vol. 17, 2016, doi: 10.1115/1.4033994.

[39] M. Pérez, D. Carou, E. M. Rubio, and R. Teti, "Current advances in additive manufacturing," *Procedia CIRP*, vol. 88, pp. 439–444, Jan. 2020, doi: 10.1016/J.PROCIR.2020.05.076.

[40] T. Singh, S. Kumar, and S. Sehgal, "3D printing of engineering materials: A state of the art review," *Mater. Today Proc.*, vol. 28, pp. 1927–1931, 2020, doi: https://doi.org/10.1016/j.matpr.2020.05.334.

[41] A. B. Varotsis, "Introduction to binder jetting 3D printing," *Hubs*, 2019. https://www.hubs.com/knowledge-base/introduction-binder-jetting-3d-printing/ (accessed Jul. 12, 2021).

[42] ExOne, "What is Binder Jetting." https://www.exone.com/en-US/Resources/case-studies/what-is-binder-jetting (accessed Sep. 06, 2021).

[43] M. Leary, "Material extrusion," *Des. Addit. Manuf.*, pp. 223–268, Jan. 2020, doi: 10.1016/B978-0-12-816721-2.00008-7.

[44] D. Systemes, "3D Printing - Additive," *3DExperience*, 2018. https://make.3dexperience.3ds.com/processes/material-extrusion (accessed Sep. 11, 2021).

[45] L. Greguiric, "What is Material Jetting - 3D Printing Simply Explained," *All3DP*, 2019. https://all3dp.com/2/what-is-material-jetting-3d-printing-simply-explained/ (accessed Sep. 02, 2021).

[46] D. Dev Singh, T. Mahender, and A. Raji Reddy, "Powder bed fusion process: A brief review," *Mater. Today Proc.*, vol. 46, pp. 350–355, Jan. 2021, doi: 10.1016/J.MATPR.2020.08.415.

[47] A. Bagheri and J. Jin, “Photopolymerization in 3D Printing,” *ACS Appl. Polym. Mater.*, vol. 1, no. 4, pp. 593–611, Apr. 2019, doi: 10.1021/acsapm.8b00165.

[48] J. Alves, “Design and Development of a Lower Limb Prosthesis,” Guimarães, 2018.

[49] H. Bateni and S. Olney, “Effect of the Weight of Prosthetic Components on the Gait of Transtibial Amputees,” *JPO J. Prosthetics Orthot.*, vol. 16, pp. 113–120, Oct. 2004, doi: 10.1097/00008526-200410000-00004.

[50] R. S. Gailey *et al.*, “Energy expenditure of trans-tibial amputees during ambulation at self-selected pace.,” *Prosthet. Orthot. Int.*, vol. 18, no. 2, pp. 84–91, Aug. 1994, doi: 10.3109/03093649409164389.

[51] B. Rochlitz, D. Pammer, and R. Kiss, “Functionality and Load-Bearing Analysis of 3D-Printed Prosthetic Feet,” *Mater. Today Proc.*, vol. 5, no. 13, pp. 26566–26571, Jan. 2018, doi: 10.1016/J.MATPR.2018.08.117.

[52] J. Yap and G. Renda, *Low-cost 3D-printable prosthetic foot*. 2015.

[53] B. Rochlitz and D. Pammer, “Design and Analysis of 3D Printable Foot Prosthesis,” *Period. Polytech. Mech. Eng.*, vol. 61, Aug. 2017, doi: 10.3311/PPme.11085.

[54] J. Nazzaro and E. Eitel, “The Benefits of Gearboxes — and When to Pick Integrated Gearmotors,” *Machine Design*, 2013. https://www.machinedesign.com/motors-drives/article/21833641/the-benefits-of-gearboxes-and-when-to-pick-integrated-gearmotors (accessed Jul. 31, 2021).

[55] C. Layosa, “Performance of Timing Belt Profiles,” *MiSUMi Mech Lab*, 2016. https://us.misumi-ec.com/blog/performance-of-timing-belt-profiles/ (accessed Jul. 31, 2021).

Appendices

A.

```
//importing required libraries

#include <Wire.h>
#include <Adafruit_MotorShield.h>
#include "utility/Adafruit_MS_PWMServoDriver.h"

Adafruit_MotorShield AFMS = Adafruit_MotorShield();
Adafruit_DCMotor *myMotor = AFMS.getMotor(1);

//setting up variables
//ReadPin is connected to the middle prong of the potentiometer
//Voltage is dependant on the position of the potentiometer, Ranges from 0 (0V) to 1023 (5V)
//Speed controls the motor, Ranges from 0 to 255 (Max)
int readPin=A1;
int Voltage;
int Speed;

void setup() {

AFMS.begin();

pinMode(readPin,INPUT);

Serial.begin(9600);

}

void loop() {

//Read Voltage value, print it, and assign it to variable

Voltage=analogRead(readPin);
Serial.println(Voltage);
delay(200);
//Three IF statements permit controling the motor's speed and direction
//If Voltage is below 400, the motor moves backwards with linearly
//increasing speed until max reverse speed is achieved, at V=0
//If Voltage is between 400 and 600, motor stops
//If Voltage is above 600 and below 1023, motor moves forwards with linearly
//increasing speed until max forward speed is achieved, at V=0

if(Voltage<=400){

  Speed=-0.6375*Voltage+255.0;
  myMotor->run(BACKWARD);
  myMotor->setSpeed(Speed);
}

else if(Voltage>400;Voltage<=600){
  myMotor->setSpeed(0);
}

else if(Voltage>600;Voltage<=1023){

  Speed=0.6028*Voltage-361.70;
  myMotor->run(FORWARD);
  myMotor->setSpeed(Speed);
}
```

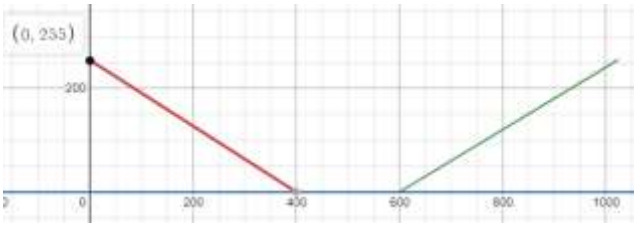

B.

DN22 Series

Iron Core【3 Slots】

DN22 M

寸法図 Dimension

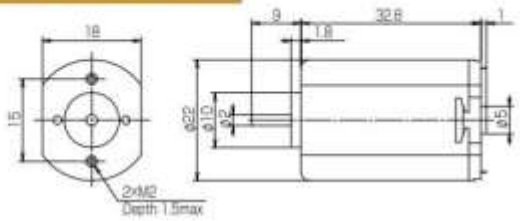

特性図 T-N-I curve

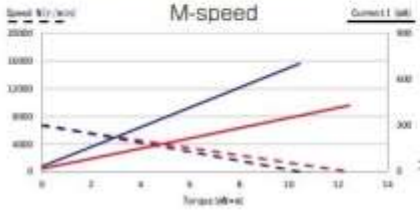

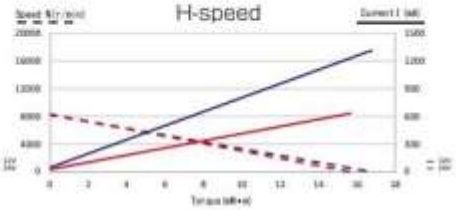

型番 Model	定格電圧 Rated Voltage	定格出力 Rated Output	定格トルク Rated Torque		定格回転数 Rated Speed	定格電流 Rated Current	無負荷回転数 No Load Speed	無負荷電流 No Load Current	起動トルク Starting Torque		起動電流 Starting Current	トルク定数 Torque Constant		端子間抵抗 Terminal Resistance (winding)	インダクタンス Inductance	イナーシャ Moment of Inertia	機械的時定数 Mechanical Time Constant	熱抵抗 Thermal Resistance	軸径 Shaft Dia	L寸 Length	質量 Weight
	V	W	mN·m	(gf·cm)	r/min	A	r/min	A	mN·m	(gf·cm)	A	mN·m/A	(gf·cm/A)	Ω	mH	g·cm²	ms	K/W	mm	mm	g
DN22 M M-speed	12	1.30	2.45	(25)	5200	0.19	6800	0.04	10.8	(110)	0.73	15.7	(160)	16.4	7.6	3.70	25.0	42.0	2.0	32.8	40
DN22 M M-speed	24	1.40	2.45	(25)	5300	0.10	6600	0.02	11.8	(120)	0.39	31.1	(317)	60.9	28.4	3.70	23.0	42.0	2.0	32.8	40
DN22 M H-speed	12	1.80	2.45	(25)	7000	0.23	8200	0.05	15.7	(160)	1.28	12.5	(127)	9.4	4.4	3.70	23.0	42.0	2.0	32.8	40
DN22 M H-speed	24	1.80	2.45	(25)	7000	0.12	8300	0.03	15.2	(155)	0.63	25.2	(257)	38.2	21	3.70	22.0	42.0	2.0	32.8	40

C.

22N28 Precious metal commutation Ø22mm 8.8 mNm

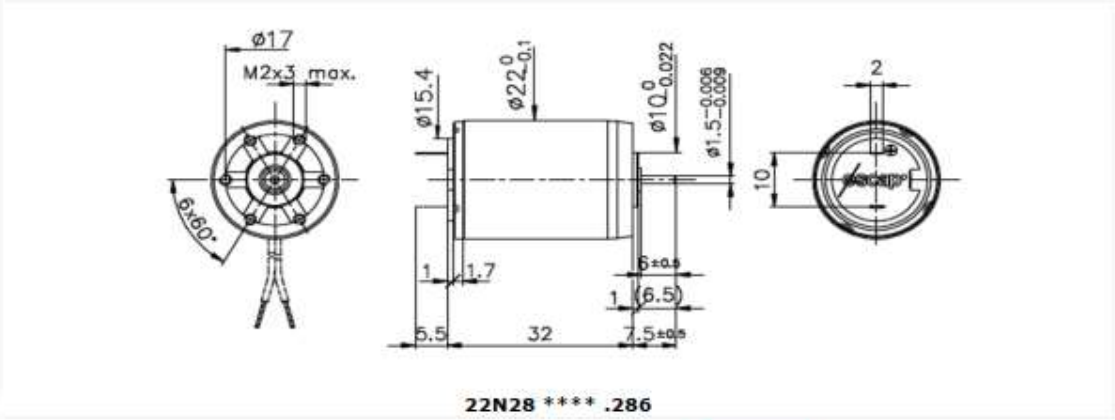

22N28 ** .286**

Electrical Data	****	216P	216E	213E	210E	208E	105	
1 Nominal Voltage	V	3	6	9	12	18	18	Volt
2 No-Load Speed	n_0	5,275	5,580	7,000	5,880	6,300	3,580	rpm
3 No-Load Current	I_0	12.6	7.0	6.0	4.5	3.5	1.4	mA
4 Terminal Resistance	R	1.5	5.8	10.3	27.0	59.0	200.0	Ω
5 Output Power	$P_{2max.}$	4.3	4.2	3.8	3.7	3.5	3.3	W
6 Stall Torque	mNm	10.9 (1.55)	10.5 (1.49)	10.7 (1.52)	8.6 (1.22)	8.2 (1.17)	4.3 (0.61)	mNm (oz-in)
7 Efficiency	$\eta_{max.}$	85	84	84	81	80	77	%
8 Max continuous speed	$n_{e\,max.}$	12,000	12,000	12,000	12,000	12,000	12,000	rpm
9 Max continuous torque	$M_{e\,max.}$	8.8 (1.19)	8.4 (1.19)	7.5 (1.07)	7.3 (1.04)	6.9 (0.98)	6.5 (0.93)	mNm (oz-in)
10 Max continuous current	$I_{e\,max.}$	1.63	0.83	0.62	0.38	0.26	0.14	A
11 Back-EMF Constant	k_E	0.57	1.07	1.28	2.02	2.83	4.95	mV/rpm
12 Torque Constant	k_M	5.40	10.20	12.20	19.30	27.00	47.30	mNm/A
13 Motor Regulation	R/k^2	51.4	55.7	69.2	72.49	80.93	89.39	10^3/Nms
14 Friction Torque	T_F	0.07 (0.01)	0.07 (0.01)	0.07 (0.01)	0.07 (0.01)	0.07 (0.01)	0.07 (0.01)	mNm (oz-in)
15 Rotor Inductance	L	0.10	0.35	0.50	1.20	2.30	7.00	mH
16 Mechanical Time Constant	τ_m	18.0	19.5	19.4	21.7	23.5	17.9	ms
17 Rotor Inertia	J	3.50	3.50	2.80	3.00	2.90	2.00	$g.cm^2$
18 Thermal Resistance (rotor/body)	R_{th1} / R_{th2}	5/20	5/20	5/20	5/20	5/20	5/20	°C/W
19 Thermal Time Constant (rotor/stator)	τ_{w1}/τ_{w2}	5/550	5/550	5/550	5/550	5/550	5/550	°C/W
20 Operating Temperature Range:	motor	-30°C to 85°C (-22°F to 185°F)						°C (°F)
	rotor	100°C (212°F)						°C (°F)
21 Shaft Load max.:		With sleeve bearings						
at 3,000 rpm (5mm from bearing)	-radial	3.0 (10.8)						N (oz)
at 3,000 rpm	-axial	150 (539.5)						N (oz)
22 Shaft play:	-radial	<0.03 (0.0012)						mm (inch)
	-axial	0.15 (0.0059)						mm (inch)
23 Weight	g	53 (1.87)						g (oz)

Execution				
Gearbox	**Single Shaft**	**F16**	**E9**	**MR2**
	22N28	**22N28**	**22N48**	**22N48**
R22	286	286	309	Contact Us
M22	286	286	308	483
K24	286	286	308	Contact Us
K27	286	286	308	Contact Us